6. Meteorological and dispersion factors governing model events in Yarloop

6.1. TAPM simulations

In this section, we investigate the meteorological and dispersion factors that lead to ground impacts of the Refinery plume in areas near the Refinery. In the NO_x modelling discussed in Section 4.2, all sources were grouped as a single tracer in TAPM and the output concentration was determined as the sum of contributions from all sources. The modelled NO_x at a particular location is generally dominated by the relatively large emissions from the Powerhouse. The post-2002 odour emission rates from the Refinery (Alcoa, 2003) suggest that the 100-m Multiflue stack and the 49-m Calciner 4 stack are the only significant point sources of odour, with the former contributing 72% (540 kilo OU s^{-1}) and the latter 26% (199 kilo OU s^{-1}) of the total point-source odour emissions. There are probably other significant sources of odour (e.g. cooling ponds) that are not accounted for in the present analysis. (Recent figures given by Alcoa after the completion of the present modelling are that the 100-m Multiflue stack and the 49-m Calciner 4 stack contribute 38% and 14%, respectively, of the total odour emissions.) Given the dominance of odour in the Wagerup complaints database, it is pertinent to examine the dispersion of plumes from these two point sources for identifying the dominant meteorological and dispersion mechanisms responsible for the Refinery plume impact in the Yarloop area. We performed TAPM simulations for the Multiflue and Calciner 4 for the same one-year period (April 2003–March 2004) as selected previously. In order to examine the differences between the dispersion patterns of plumes from the two sources, the two-tracer mode option in TAPM was selected so that the concentration output for each source could be obtained separately. The odour emission rates with the source proportions given above were used. The other model settings were the same as in Run B for the NO_x modelling. The hourly-averaged TAPM odour concentrations at ground level in Yarloop (model AMG coordinates 397.600 km east and 6354.000 km north) due to the two sources were analysed.

For the purposes of the present analysis, a model event (or exceedence) was defined as an occurrence when the hourly-averaged model concentration is greater than a threshold concentration level of 0.1 Odour Unit (OU). Because of model structure, this threshold corresponds to an hourly-average concentration over a grid cell of 250 m × 250 m × 10 m. *It is stressed that the present definition of an event is arbitrary, and is adopted solely to ensure that there is an adequate frequency of model events (i.e. sample size) for the purpose of investigating the trends in the frequency with respect to various meteorological factors.* The present model event definition can differ from odour event definitions prescribed for regulatory applications. The sensitivity of the distribution of model events to the odour threshold value selected is presented in the next section.

An Odour Unit of one (a concentration that will be discerned as odorous by approximately half the population) or larger is usually taken as the threshold level for regulatory odour assessment. However, this threshold is applicable to typical odour events that occur over short-time periods (e.g. 1–3 min), and concentrations during these events can be an order of magnitude larger than hourly-averaged concentrations. Our threshold value is applied to the hourly-averaged concentration, and is, therefore,

smaller. A model that provides a near-instantaneous concentration time series is required for determining the statistics of short-term events with better accuracy.

6.2. Diurnal variation of model events

The average diurnal variation of the percentage occurrence of the model events over the period April 2003–March 2004 in Yarloop obtained from TAPM is presented in Figure 27. It is possible to make a qualitative comparison of the model variation with the diurnal variation of the number of complaints in the local area. The Alcoa Wagerup complaints data (file "ccs.xls") for the period March 2000–March 2003 were filtered to include only the "Caustic Mist", "Fumes", "Health Issues" and "Odour" category complaints, and then grouped by hour of complaints. Figure 27 shows the variation of the percentage occurrence of complaints thus obtained. (A similar model analysis was reported by CSIRO (2004d) for the winter period May–August 2002.) Although the model simulation period and the complaints period are not exactly the same, and the Refinery source configuration was somewhat different prior to July 2002, there is a good degree of correspondence between the model event variation and the variation of the number of complaints. The highest number of model events occurs in the late morning at 1000 h, which is consistent with the peak in the complaints number. The morning peak in complaints number was observed in the analyses conducted by CSIRO (2004d), SKM (2002), and Riley (2002). In Figure 27, there is a secondary peak in the complaints number at 1900 h, which the model does not predict very well. There are some nighttime model events, but not seen in the complaints pattern, presumably because most people are indoors/asleep. Overall, the comparison shows qualitative agreement. In addition to meteorological and emission factors, the complaints pattern is probably also influenced by the diurnal pattern of the activities of the residents and the sensitivity of their olfactory and other sensors. However, it is instructive to identify the meteorological factors responsible for the model events.

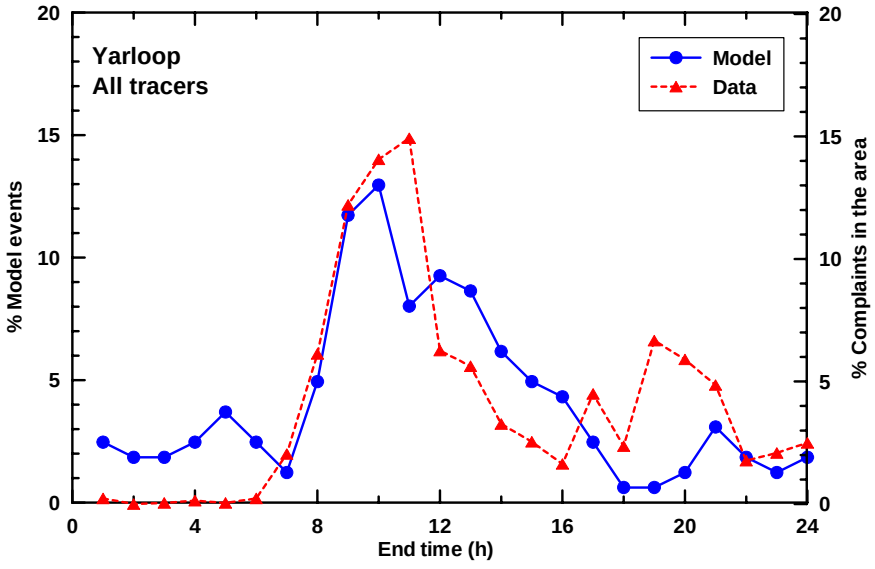

Figure 27: Diurnal variation of the percentage complaints in the local area around the Wagerup Refinery (mostly Yarloop) and that of the percentage model events in Yarloop.

Figure 28 shows the diurnal variation of the number of model events (or exceedences) for the 100-m Multiflue, Calciner 4, and both sources. Generally the main morning peak

is dominated by the Multiflue Stack. For the late afternoon and night period between 1800–0400 h, Calciner 4 generally causes a larger number of model events than the Multiflue, even though the emissions from Calciner 4 are only about third of those from the Multiflue. This is because the plume from the Multiflue Stack is too high to contribute at the ground at these times when the vertical plume diffusion is limited due to the neutral/stable stability. However, during 0400–0700 h the number of model events from Multiflue is greater, largely because of the drainage flow from the escarpment coupled with the turning of the wind with height that cause high plume diffusion and the consequent mix-down of the Multiflue plume to the ground (see Section 6.3.3).

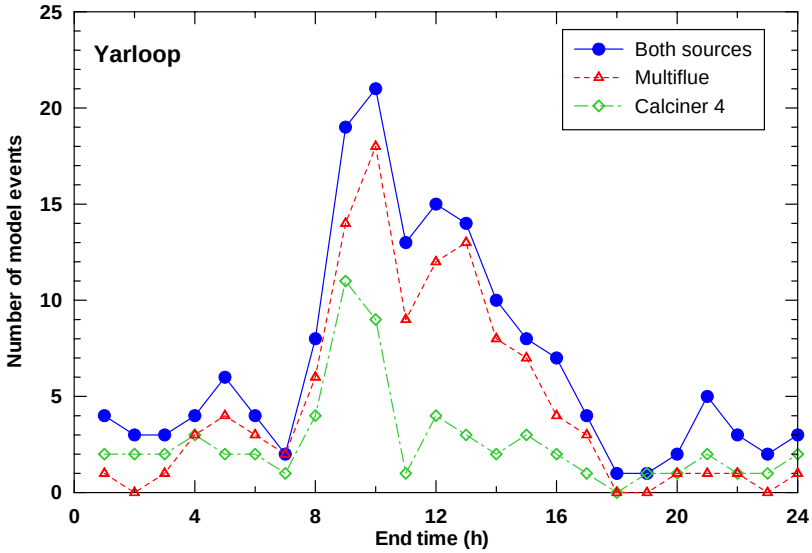

Figure 28: Diurnal variation of the percentage model events in Yarloop due to the dominant refinery stacks.

Figure 29 demonstrates that the qualitative shape of the diurnal distribution of the relative frequency of model events is fairly insensitive to the odour threshold value selected for defining a model event. When the odour threshold value is decreased to 0.05 OU, the distribution becomes slightly flatter. However, when the threshold value is increased progressively, the main peak of the distribution becomes more and more pronounced, with some night events disappearing and some daytime peaks becoming bigger. Of course, the absolute number of events varies considerably with the threshold value selected. With a threshold value of 0.1 OU, there are a total of 162 model events (due to the two stack odour sources considered) at the Yarloop location within the model year. There is a 50% increase in the number of events when the odour threshold value is lowered from 0.1 OU to 0.05 OU, and there is about 40% and 65% decrease when the odour threshold value is increased to 0.2 OU and 0.3 OU, respectively.

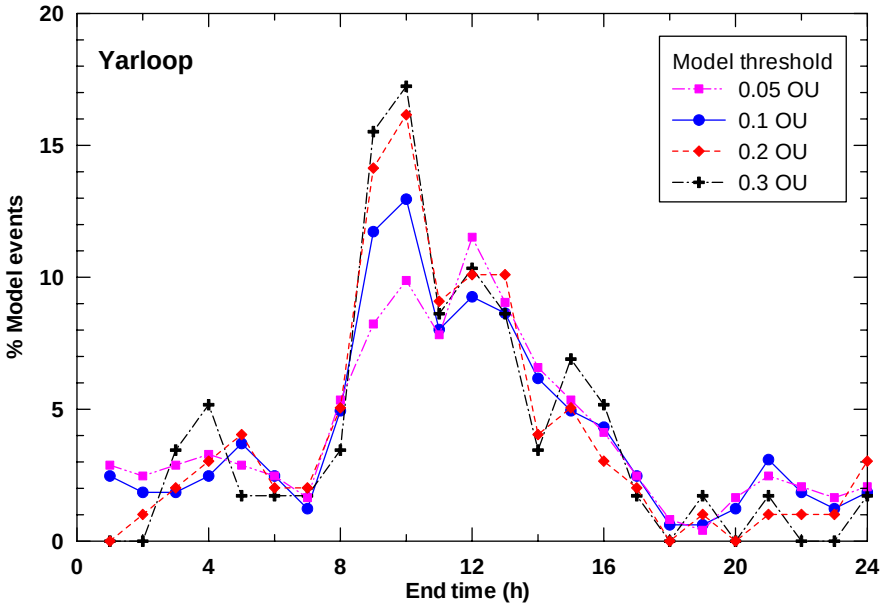

Figure 29: Sensitivity of the diurnal distribution of percentage model events on the odour threshold value selected in Yarloop.

The broad meteorological and dispersion mechanisms that lead to model events of concentration greater than 0.1 OU, specifically in the Yarloop area, are considered in the next section.

6.3. Factors governing model events

The hourly-averaged 10-m wind directions at Bancell Road predicted by the model when there are model events are plotted against the diurnal time in Figure 30. Most model events occur when the wind is northerly, so that Yarloop is directly downwind of the Refinery. Under such conditions, model events can occur anytime of the day. Generally, these are the *only* conditions that would be identified by a Gaussian plume model such as AUSPLUME. There are also cases when model events occur under easterly winds in the nighttime and under westerly winds in the daytime. The turbulent dispersion conditions leading to these model events are described below.

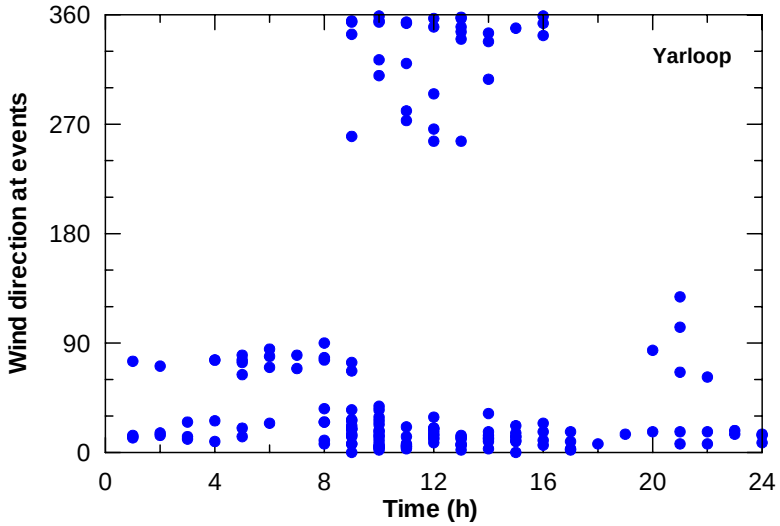

Figure 30: Model 10-m wind directions at Bancell Road at the time of model events as a function of time.

The frequency of model events plotted as a function of wind direction in Figure 31 shows that winds between 330°–30° lead to the highest number of model events, followed by ENE and winds with a north-westerly component.

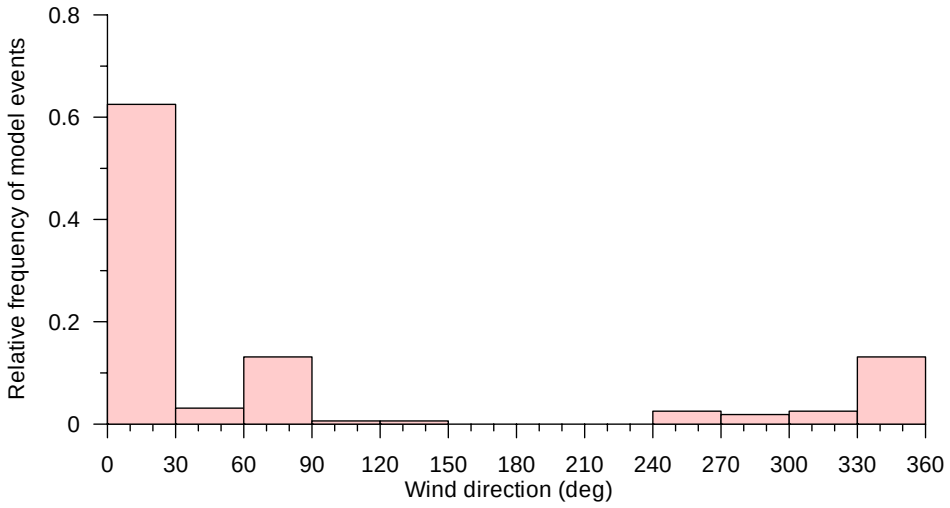

Figure 31: Normalised frequency of model 10-m wind direction at Bancell Road when there are model events.

The variation of the intensity of the model events, defined as the model concentration scaled by the peak concentration value from the set of all events, presented in Figure 33 as a function of the diurnal time shows that most intense events occur in the late morning. This is also the time when the events are most frequent (see Figure 27). The variation of the intensity of the model events as a function of the modelled 10-m wind direction at Bancell Road in Figure 32 indicates that most intense events occur when the surface wind is northerly.

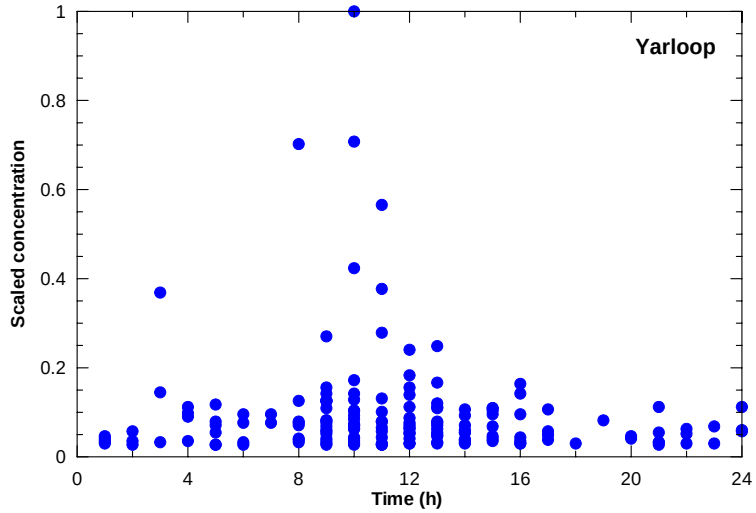

Figure 32: Variation of the model concentration scaled by the peak value at the time of model events as a function of time.

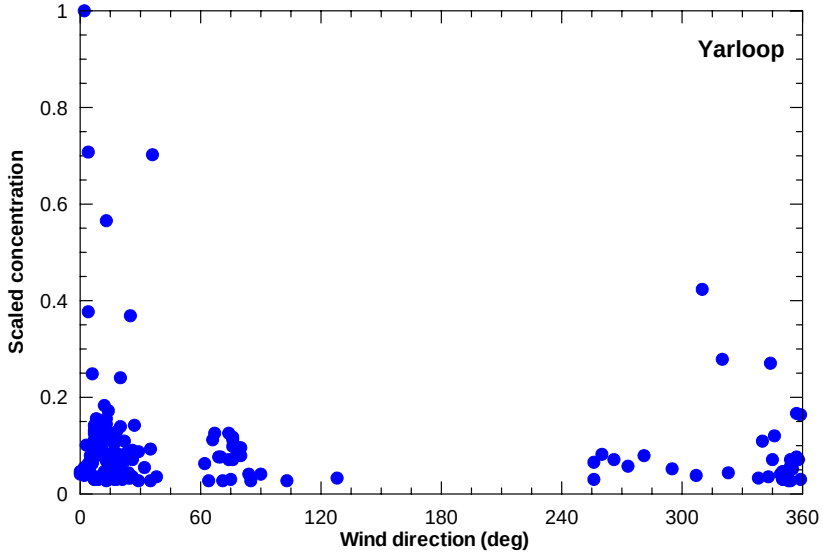

Figure 33: Variation of the model concentration scaled by the peak value with the modelled 10-m wind direction at Bancell Road at the time of model events.

It is estimated that about 77% of the model events at Yarloop occur for model wind direction between 330°–60° when the Yarloop area is downwind of the Refinery. These events are dominated by fumigation, shallow convective mixing and near-neutral atmospheric stability. About 15% of the model events that occur for model wind direction between 60°–150° are dominated by wind shear and nocturnal drainage flow conditions, while 8% of the model events that occur for model wind direction between 240°–330° are dominated by low/calm wind speed conditions. These are discussed below.

6.3.1 Late morning model events: fumigation and shallow convective mixing

The late morning model events at Yarloop generally occur when the area is directly downwind of the Refinery under the conditions of anticlockwise turning of the wind with time. Figure 34 shows an example of this situation on 25 July 2003. In this figure, the top solid square in the centre represents the Refinery source location, the middle one the Bancell Road meteorological monitoring site, and the bottom one the Yarloop township. The meteorological grid domain is 15 km × 15 km, whereas the dispersion grid domain is 6 km × 6 km. At 0900 h, only a small part of the plume reaches the ground (Figure 34a) and the ground level concentrations are relatively low (there was no plume portion reaching the ground during the hour prior to this). However, at 1000 h the plume has impacted the ground with sufficiently high concentrations to cause a model event (Figure 34b). At 1100 h and 1200 h, the ground-level concentrations remain high but the turning of the wind with time moves the plume away from the town (Figure 34c and Figure 34d).

There are two mechanisms by which an elevated plume can reach the ground in the morning. The first is the transient event (~30 min) called the nocturnal inversion break-up fumigation, in which an elevated point-source plume travelling in nighttime stable flow with little diffusion is intercepted by the growing convective mixed layer (with inversion aloft) that develops in the morning as a result of the heating of the ground by solar radiation. The plume is subsequently mixed down to the ground by the large-scale convective eddies generated within the mixed layer. The schematic diagram in Figure 35 shows a spatial pattern of the nocturnal inversion break-up fumigation at a given instant, while that in Figure 36 presents a temporal evolution of the nocturnal inversion break-up fumigation at a given location downwind of the source.

Nocturnal inversion break-up fumigation is a transient event, whereas TAPM output concentrations are hourly averages. TAPM calculates the values of ensemble-averaged flow, turbulence and pollution quantities at every model time step. The time step used in TAPM calculations depends on the grid size, the variables being calculated and the selected model options. For the innermost grid resolution of 0.5 km used in this work, the TAPM time step is about 17 seconds for the meteorological and turbulence quantities. For the pollution calculations for the innermost grid, the model time step is 1 second for the solution of plume rise equations, 34 seconds in the horizontal and 5 second in the vertical for the Lagrangian particle dispersion module, and 17 seconds for the Eulerian dispersion module. With such short time steps, which are required to solve the model differential equations accurately, the model is able to resolve the ensemble-average fumigation process in the computations. However, the model only outputs hourly-averaged concentrations, not the sub-hourly (e.g. 15-min average) concentrations fields that resolve the fumigation evolution better. The hourly concentrations only include the averaged effects of fumigation. While it is necessary to carry out all these calculations at these short time steps in order to reliably do the numerical calculations, the physics of the model is optimised to predict hourly-average meteorological and concentration fields rather than those for shorter time periods.

The second mechanism is convective mixing, which occurs subsequent to fumigation when the convective mixed-layer is deep enough such that the plume is released and dispersed within this layer. Convective mixing can last as long as there is sufficient

heating of the ground. The same large-scale convective eddies generated within the mixed layer cause the plume to impact at ground level with relatively high concentrations. At Yarloop, convective mixing largely occurs in the morning subsequent to fumigation when the town is still directly downwind of the Refinery. At this time, the convection is shallow, and the mixing is not as strong as that occurs under fully-developed convection in the early afternoon (when the town is not downwind of the Refinery). Figure 37 shows a schematic diagram of plume dispersion under shallow convection conditions in which diffusion is caused by both mechanically-generated turbulent eddies and the convective eddies within a shallow convective boundary layer (or mixed layer). The plume also undergoes some bodily motion in the vertical direction due to the larger-sized convective eddies.

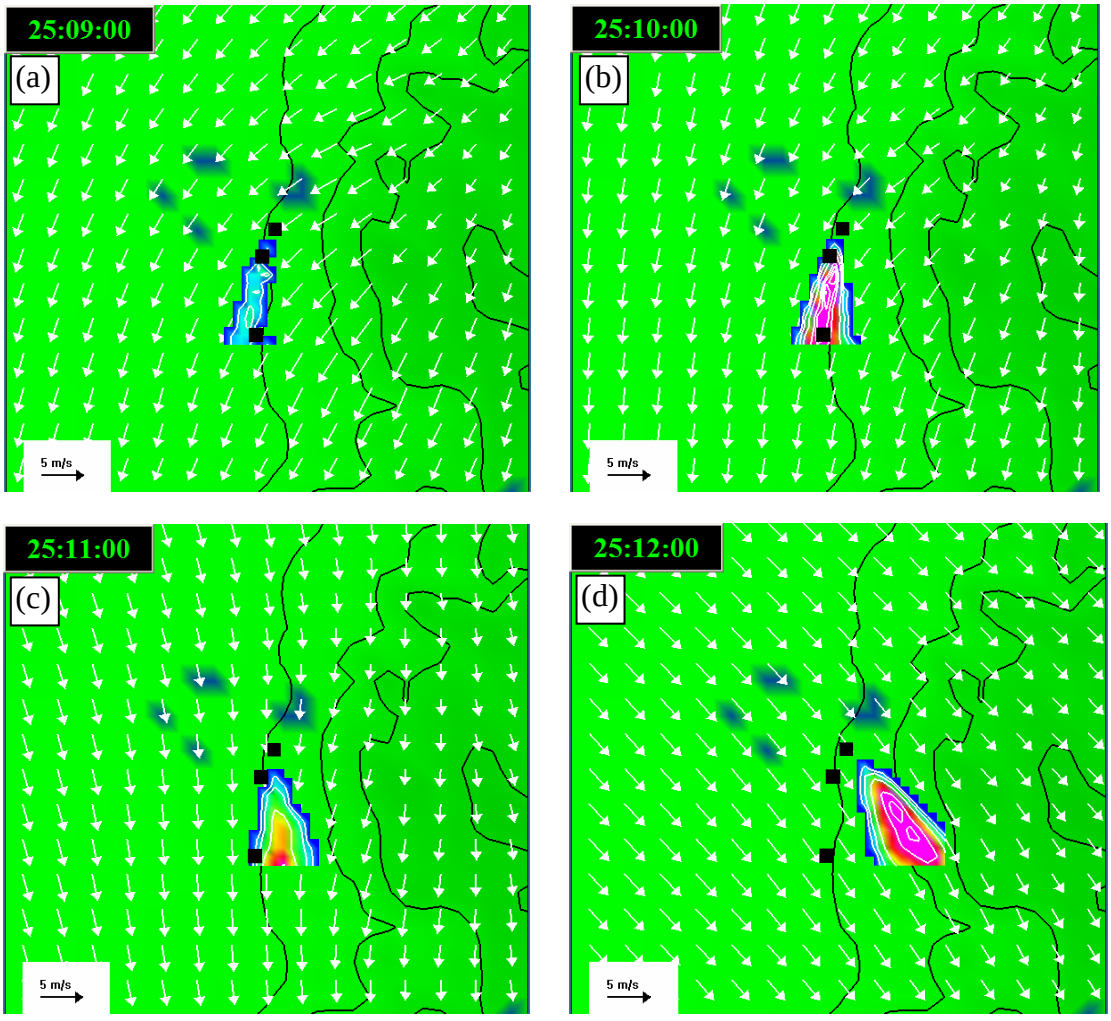

Figure 34: Model 10-m wind fields and concentration contours on 25 July 2003 at (a) 0900 h, (b) 1000 h, (c) 1100 h, and (d) 1200 h. The meteorological grid domain is 15 km × 15 km, whereas the dispersion grid domain is 6 km × 6 km. The top solid square in the centre represents the Refinery source location, the middle one the Bancell Road meteorological monitoring site, and the bottom one the Yarloop township. The four blue areas north/north-west of the Refinery are water bodies. The black lines are the topographical contours of 50, 100, 200 and 300 m above mean sea level, increasing in elevation from left to right.

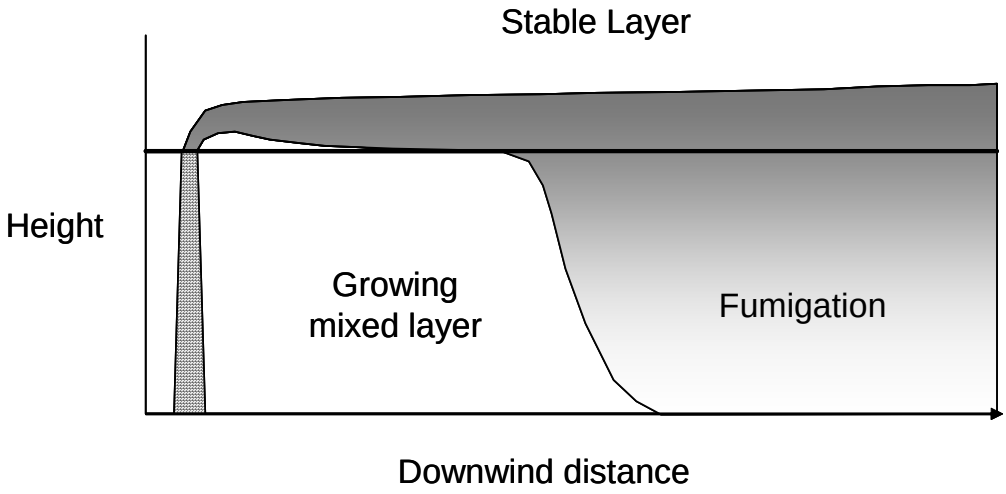

Figure 35: Schematic diagram of the spatial pattern of the nocturnal inversion break-up fumigation at a given instant.

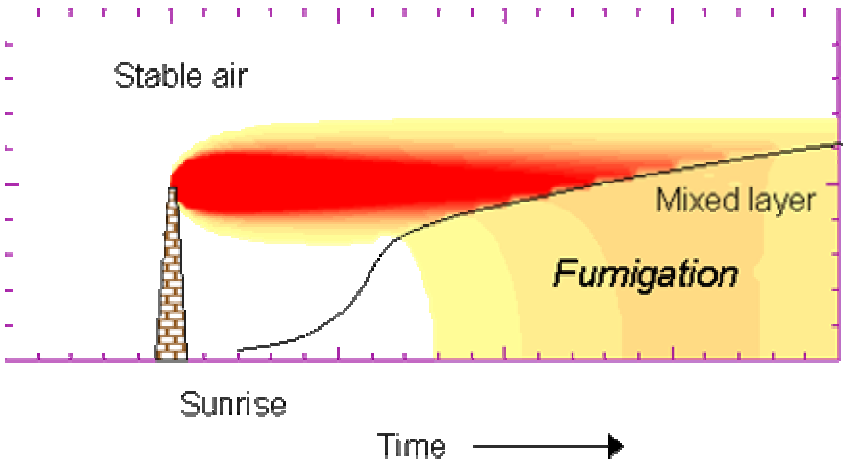

Figure 36: Schematic diagram of the temporal evolution of the nocturnal inversion break-up fumigation at a given location downwind of the source.

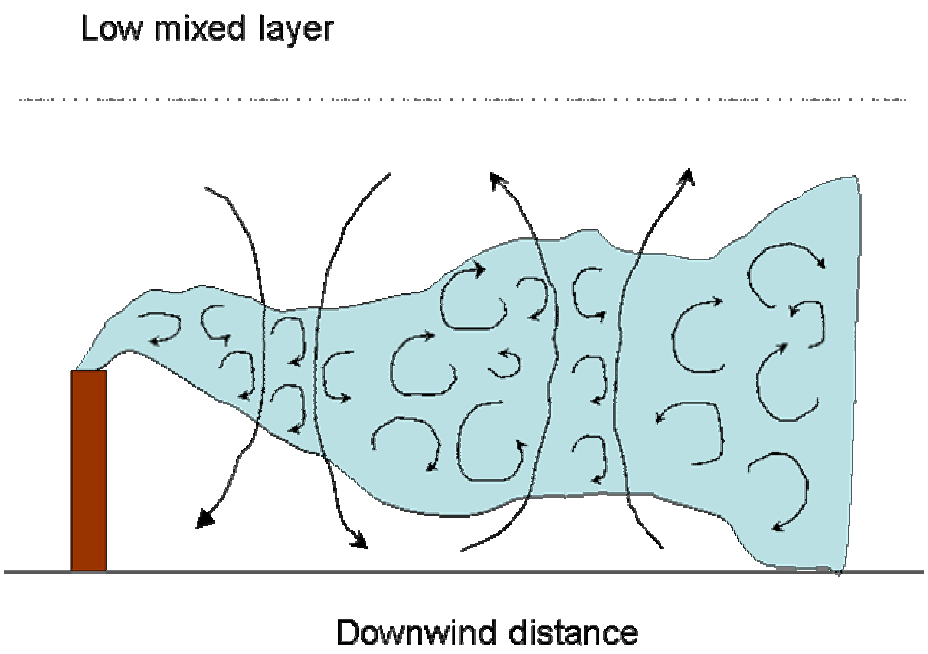

Figure 37: Schematic diagram of plume dispersion under shallow convection conditions. The plume diffusion is caused by both mechanically-generated turbulent eddies and the convective eddies produced by the solar heating of the ground. The plume also undergoes some bodily motion in the vertical direction due to the larger-sized convective eddies.

6.3.2 Near-neutral atmospheric stability

There are also model events when Yarloop is directly downwind of the Refinery and the atmospheric stability is neutral or near neutral. Near-neutral stability occurs both by day or night when the winds are strong and there are clouds, resulting in no significant heating or cooling of the ground. Under such conditions, the frictional drag imposed on the strong winds by the ground produces enhanced mechanical turbulence that can diffuse an elevated stack plume to the ground, causing high ground-level concentrations. (On the other hand, under strongly stable, inversion conditions with weaker winds in the nighttime, the intensity of mechanical turbulence is very small, and, consequently, an elevated plume diffuses very slowly vertically with low ground-level concentrations.) The intensity of mechanical turbulence, which is composed of mainly small eddies, increases with the roughness of the surface and the wind speed. Because of the small size of turbulent eddies compared to the size of the plume size, the plume mostly grows by diffusion with little transport in the vertical direction (see Figure 38). Figure 39 shows such a situation predicted by TAPM at 2100 h on 29 May 2003.

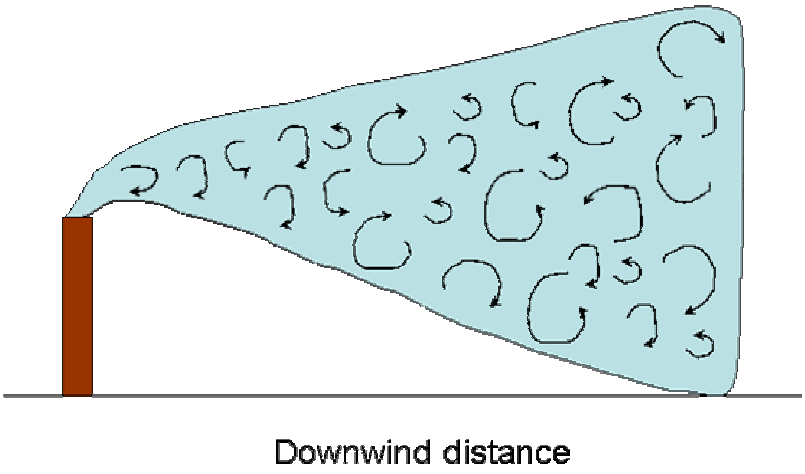

Figure 38: Schematic diagram of plume dispersion under near-neutral conditions. The plume diffusion is caused mainly by the small-scale, mechanically-generated turbulent eddies, with the plume undergoing little bodily motion in the vertical direction.

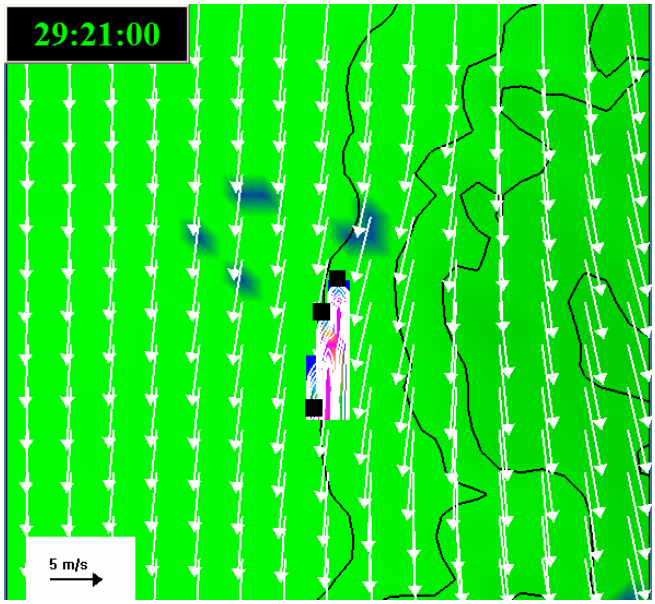

Figure 39: Model 10-m wind fields and concentration contours at 2100 h on 29 May 2003. The meteorological grid domain is 15 km × 15 km, whereas the dispersion grid domain is 6 km × 6 km. The top solid square in the centre represents the Refinery source location, the middle one the Bancell Road meteorological monitoring site, and the bottom one the Yarloop township. The four blue areas north/north-west of the Refinery are water bodies. The black lines are the topographical contours of 50, 100, 200 and 300 m above mean sea level, increasing in elevation from left to right.

6.3.3 Wind shear and nocturnal drainage flow

In this section, the causes for model events during the night under easterly surface winds are investigated. A typical day is 7 August 2003 when TAPM indicates nighttime model events at 0400 h. Figure 40a shows the surface (i.e. 10 m AGL) wind field and concentration distribution (due to emissions from both modelled stacks, as before)

calculated by TAPM. The surface flow from the escarpment is almost easterly and weakens as it goes past the Refinery. Figure 40b is the same as Figure 40a except that the winds calculated at the 150-m level are shown. The winds at this level are weaker than the surface winds, and are from the north/north-west. Hence, it is clear that the surface winds are nocturnal drainage (or downslope) flows from the escarpment due the differential cooling of the ground causing the lower air layers to cool, increase in density, and slide down the slope under the influence of gravity. Therefore, a plume released from an elevated source to within 150 m from the ground would disperse under the influence of changing wind direction (i.e. wind direction shear). The plume would experience low wind speeds in an air layer in which the upper level flow almost equally opposes the lower-level drainage winds. Both wind direction shear and low wind speeds would cause an enhanced horizontal spreading the plume, which may lead to high ground-level concentrations. The plume concentration distribution shown in Figure 40a and Figure 40b demonstrate this enhanced spreading. The north-westerly airflow within which the elevated stacks release emissions, initially transports the plume south-east of the refinery, and subsequently the lower parts of the plume are entrained into the low-level easterly/north-easterly drainage flow, causing model events in Yarloop. This is shown in a schematic diagram in Figure 41.

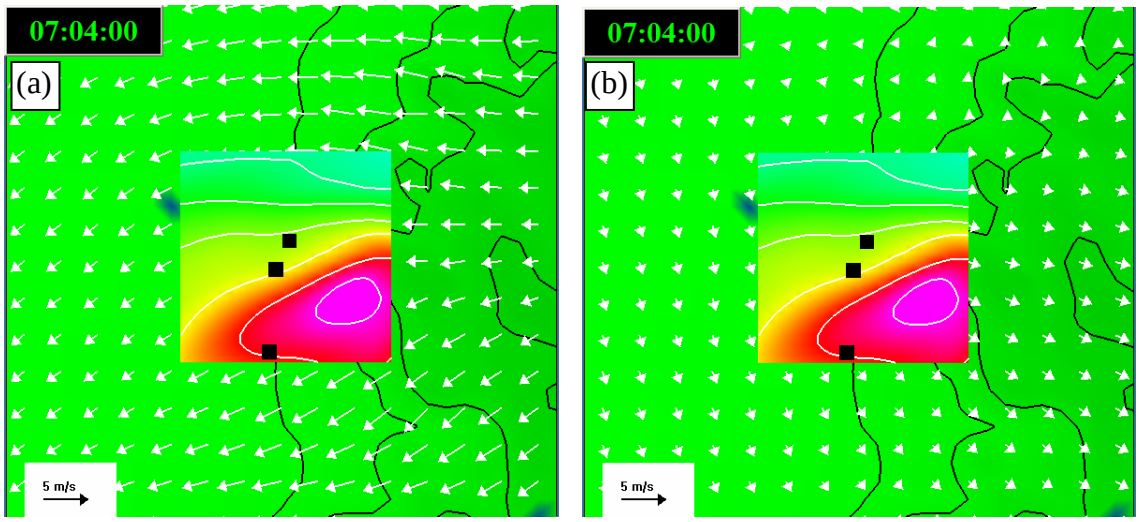

Figure 40: Model wind fields and surface concentration contours at 0400 h on 7 August 2003. The winds in (a) are at 10 m AGL, whereas in (b) they are at 150 m AGL. The meteorological grid domain is 15 km × 15 km, whereas the dispersion grid domain is 6 km × 6 km. The top solid square in the centre represents the Refinery source location, the middle one the Bancell Road meteorological monitoring site, and the bottom one the Yarloop township. The four blue areas north/north-west of the Refinery are water bodies. The black lines are the topographical contours of 50, 100, 200 and 300 m above mean sea level, increasing in elevation from left to right.

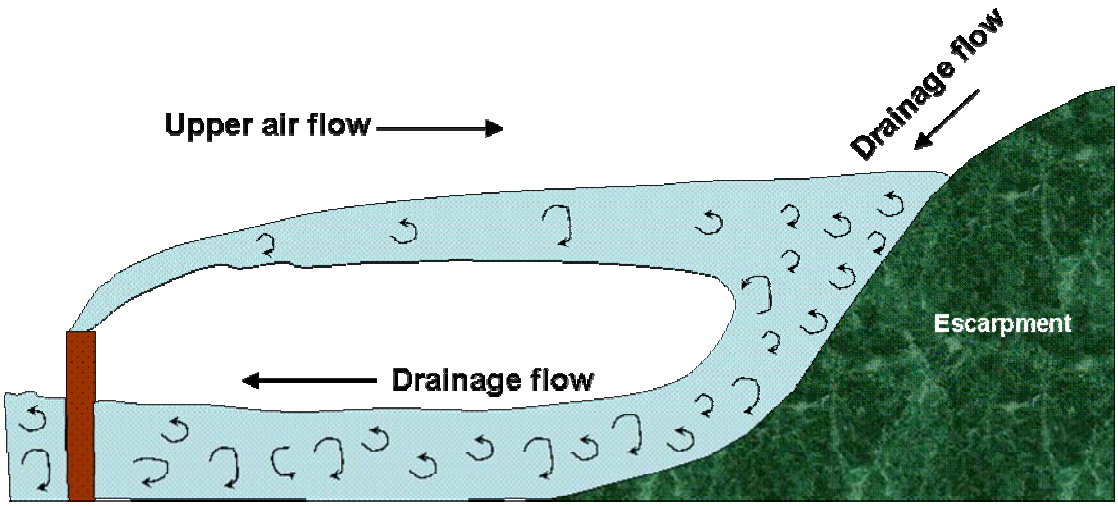

Figure 41: Schematic diagram of plume transport and diffusion under nocturnal drainage flow conditions. The diffusion is caused mainly by plume buoyancy and wind shear.

6.3.4 Daytime low wind speeds

In Figure 30, some of the model events that occur under westerly winds are caused by low winds during the daytime. Under such conditions, an instantaneous plume released from a chimney remains narrow and undergoes a high degree of horizontal meander. When these instantaneous plumes are averaged over hourly intervals (e.g. the averaging time in TAPM), the size of the averaged plume footprint can be quite large due to the large spatial coverage of the instantaneous plume meandering (see Figure 42).

Figure 43a shows the model predicted surface winds and concentration distribution at 1100 h on 7 February 2004. The enhanced horizontal diffusion caused by the low wind speeds is evident, with a relatively large areal coverage. Although the surface winds are westerly, the plume direction in Figure 43a suggests north-easterly winds. This is because the plume transport is influenced by the flow during the previous hour, which was north-easterly. Low-wind model events can also occur under different surface wind directions; for example Figure 43b at 1400 h on 18 July 2003.

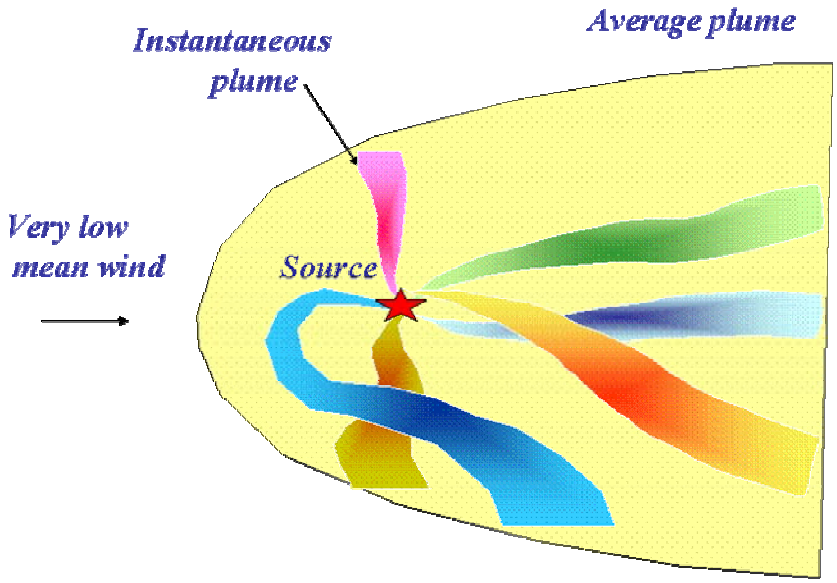

Figure 42: Schematic diagram of horizontal plume transport and diffusion under low mean speed conditions. The instantaneous plume is characterised by a narrow width and a high degree of meandering. However, the width of the averaged (e.g. hourly) plume can be relatively large due to the large spatial coverage by the meander of the instantaneous plume.

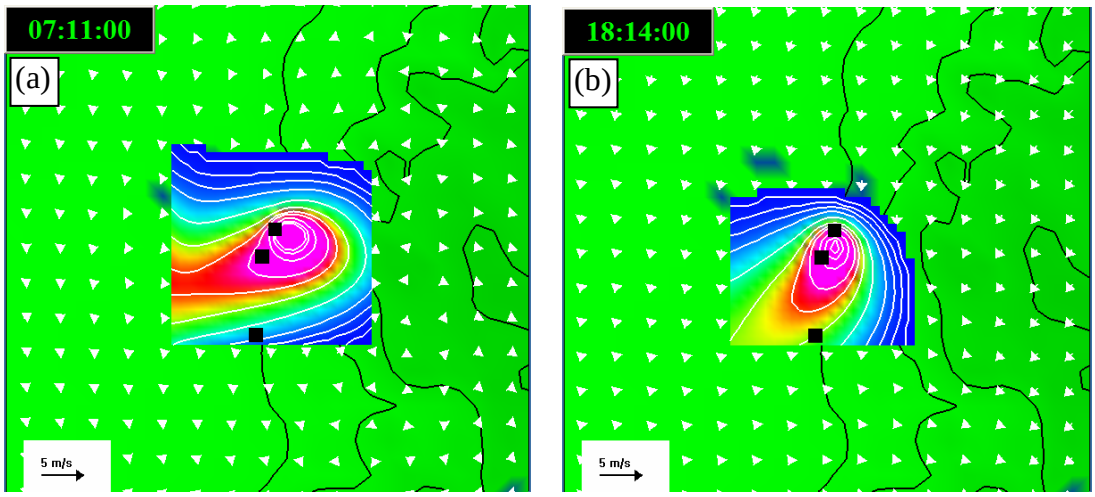

Figure 43: Model 10-m wind fields and concentration contours at (a) 1100 h on 7 February 2004, and (b) 1400 h on 18 July 2003. The meteorological grid domain is 15 km × 15 km, whereas the dispersion grid domain is 6 km × 6 km. The top solid square in the centre represents the Refinery source location, the middle one the Bancell Road meteorological monitoring site, and the bottom one the Yarloop township. The four blue areas north/north-west of the Refinery are water bodies. The black lines are the topographical contours of 50, 100, 200 and 300 m above mean sea level, increasing in elevation from left to right.

6.4. Meteorological conditions during model events

6.4.1 Wind speed

The model 10-m wind speeds at Bancell Road at the time of model events, plotted as a function of time in Figure 44, show that the model events occur under a wider range of wind speeds in the daytime period (0800–1800 h) than in the nighttime.

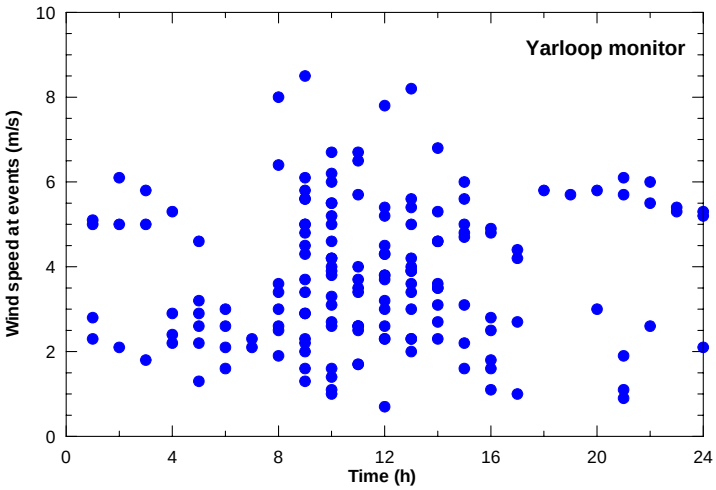

Figure 44: Model 10-m wind speeds at Bancell Road at the time of model events as a function of time.

The frequency histogram of model events plotted as a function of wind speed in Figure 45 shows that most model events occur under moderate winds between 2–6 m s^{-1}, followed by wind speeds under 2 m s^{-1}.

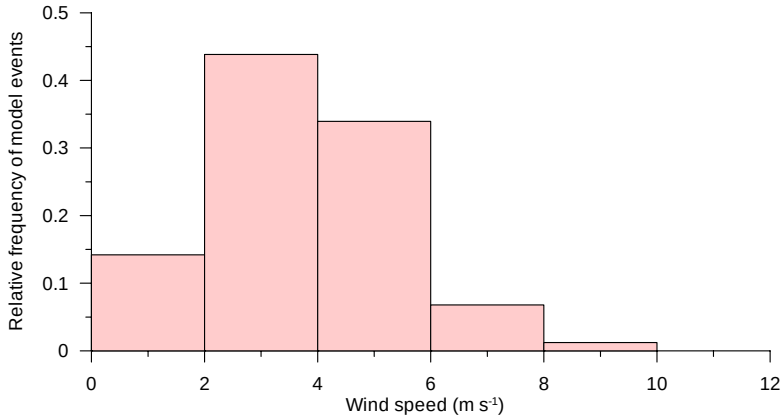

Figure 45: Normalised frequency of model 10-m wind speed at Bancell Road when there are model events.

The model 10-m wind speeds at Bancell Road at the time of model events, plotted as a function of wind direction at the same level in Figure 46, show that the model events occur under a wide range of wind speeds when the town is downwind of the Refinery. Wind speeds are relatively low for the model events that occur when the flow is

easterly. For the model events that occur when the flow is westerly, the wind speed is low to moderate.

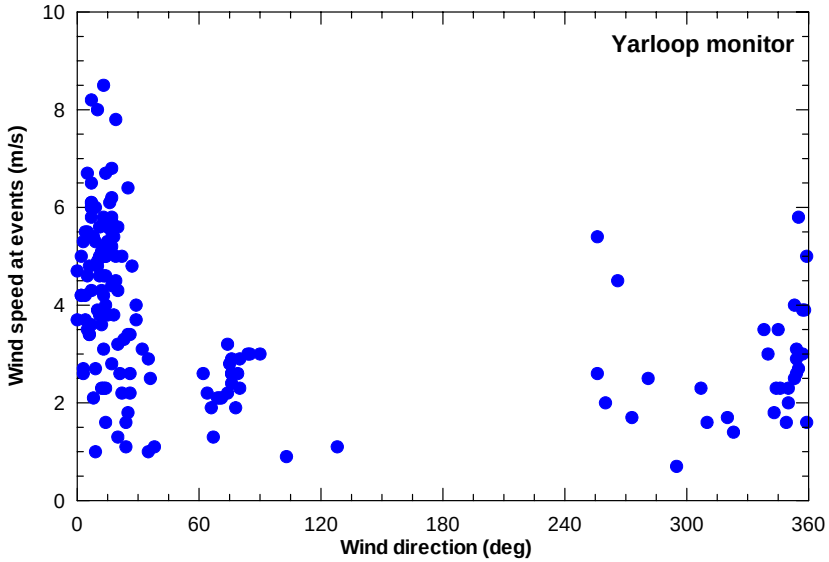

Figure 46: Model 10-m wind speed at Bancell Road as a function of wind direction at the same level at the time of model events.

An analysis of the number of complaints as function of observed 10-m Bancell Road wind speed and wind direction was carried out by SKM (2002) using data from three months April–June 2001. Complaints are received from areas other than Yarloop (e.g. Hamel and Waroona, north of the Refinery), but most complaints are from Yarloop, especially in the wintertime when Yarloop is frequently downwind of the Refinery. There is a qualitative similarity between the model event trends in Figure 30, Figure 44, and Figure 46, and the complaint trends given in SKM (2002), even though the periods and the pertinent Refinery sources in the two analyses are different. As an example, Figure 47 from SKM (2002) shows the plot of the observed wind speed vs. the observed wind direction at the time of complaints (a wind speed of 15 km/hr is approximately equal to 4 m s^{-1}), which can be compared with the plot for model events in Figure 46. This similarity between the behaviour of the complaints and the behaviour of the model events suggests that the model is realistically simulating, in qualitative terms, the dominant physical processes that potentially link the frequency of complaints in Yarloop with the meteorology of the area.

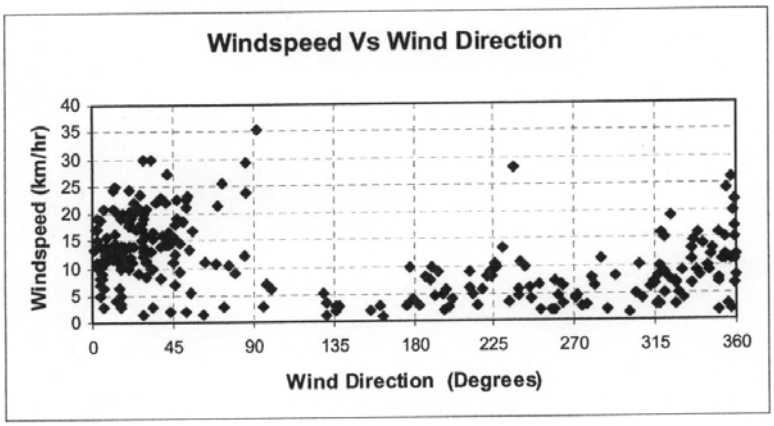

Figure 47: Observed 10-m wind speed at Bancell Road as a function of wind direction at the same level at the time complaints (from SKM, 2002).

6.4.2 Atmospheric stability

The vertical stability of the atmosphere directly influences the amount of vertical diffusion of a plume. *Neutral* stability arises when winds are strong and/or when there is a negligible heating or cooling of the ground (i.e. near-zero surface heat flux). The latter conditions occur during overcast conditions. A stack plume released within neutral atmosphere diffuses by mechanical turbulence. The atmosphere is *stable* during the night when the ground is substantially cooler than the air above it (i.e. heat flux down into the surface), thus causing a stable density-stratification to develop. Consequently, the vertical diffusion is suppressed and a plume or puff of pollutant dilutes very slowly during its transport downwind. *Unstable* stability occurs during the day with low to moderate wind speeds, and clear to partly cloudy conditions. The ground is warmer than the surrounding air (i.e. heat flux up from the surface), giving rise to relatively large convective turbulent motions in the vertical direction, which are termed thermals (or updrafts) and downdrafts. A plume released in the convective boundary layer (CBL) undergoes meandering (also called looping) and high diffusion as a result of large-scale convective motions.

For dispersion calculations stability is classified into categories, known as the Pasquill-Gifford (PG) stability categories: A (extremely unstable), B (moderately unstable), C (slightly unstable), D (neutral), E (slightly stable) and F (stable).

The model stability types at Bancell Road at the time of model events, plotted as a function of time in Figure 48, show that model events can occur at any time of the day when the stability is D (neutral). Model events under unstable stability occur during the period 0800–1700 h. Nighttime model events occur under both E and F categories. The F-category model events mainly occur under the influence of downslope flow from the escarpment.

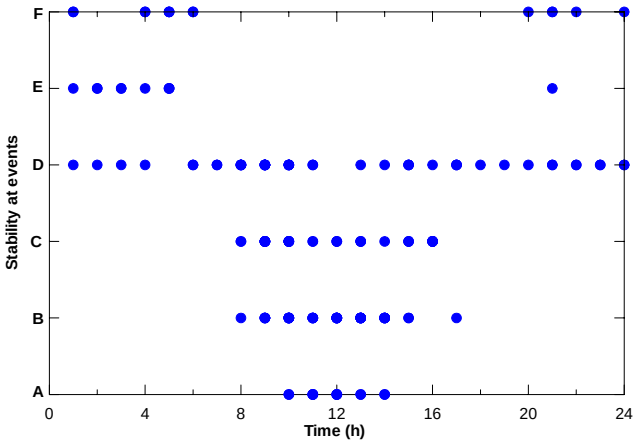

Figure 48: Model atmospheric stability at Bancell Road at the time of model events as a function of time.

The frequency of model events plotted as a function of stability in Figure 49 shows that most model events occur under neutral, moderately unstable, and slightly unstable conditions.

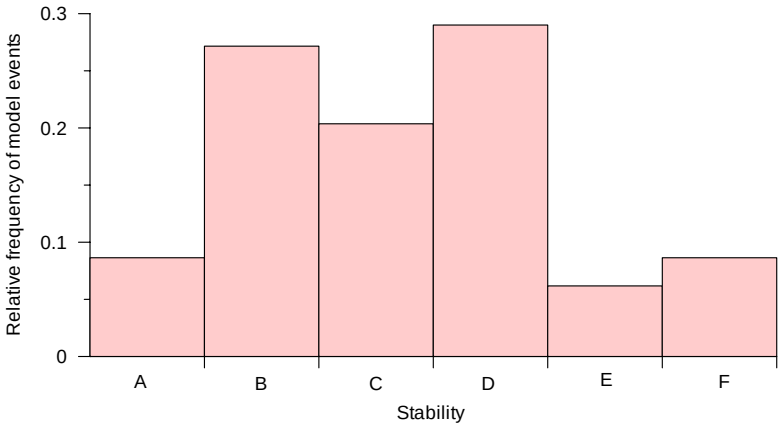

Figure 49: Normalised frequency of model atmospheric stability at Bancell Road when there are model events.

6.4.3 Boundary-layer height

The model boundary-layer height at Bancell Road at the time of model events plotted as a function of time in Figure 50 shows that model events can occur under the full diurnal range of the boundary-layer height, with most model events occurring when the boundary-layer height is less than 500 m. The frequency of model events plotted as a function of boundary-layer height in Figure 51 shows that the event frequency decreases as the boundary-layer height increases. It should be noted that the lower frequency of model events for a higher value of boundary-layer height does not necessarily mean that that value allows only a relatively small concentrations at the ground; more often, in the present context, it means that the town is not downwind of the Refinery under the conditions when boundary-layer heights are large.

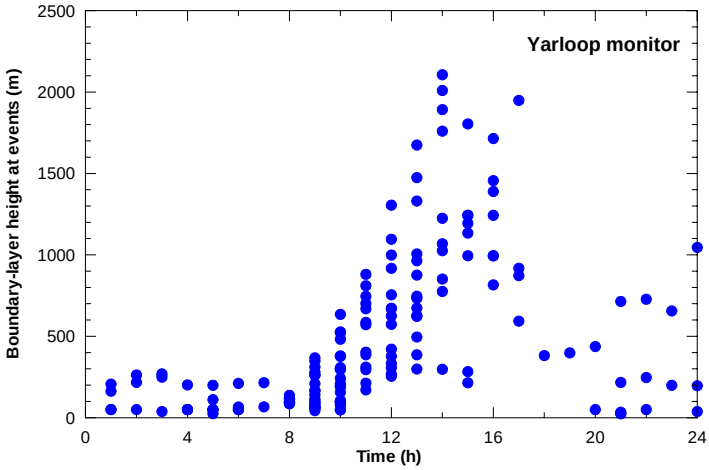

Figure 50: Model boundary-layer height at Bancell Road at the time of model events as a function of time.

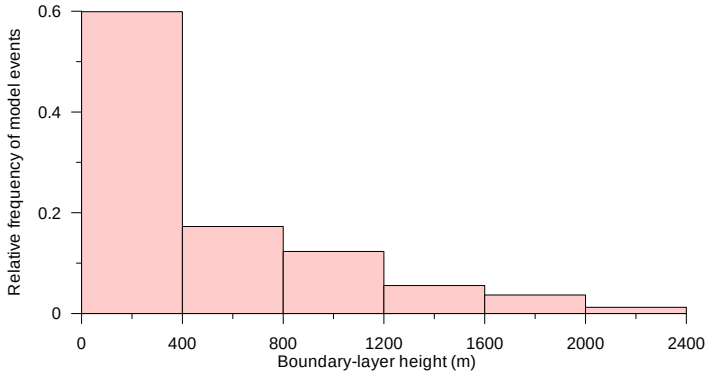

Figure 51: Normalised frequency of model boundary-layer height at Bancell Road when there are model events.

The above event analysis is based on the modelling results for Yarloop. The diurnal variation of the number of model events is supported by the results from the complaints analysis. The atmospheric conditions leading to model events may be different for northern areas (e.g. Hamel and Waroona). The analysis of modelled and observed winds for the one-year period April 2003–March 2004 reported in CSIRO (2004a) shows that southerly winds are more frequent than northerly winds. Therefore, it is possible that the number of model events north of the Refinery is potentially higher than in the areas south of the Refinery in a year. But, because the northern receptors are further from the Refinery than Yarloop, the frequency of model events at these locations may, still, be smaller than at Yarloop. In general, the reported frequency of observed events also depends on the population of an area.

The analysis of model events described above is based on hourly-averaged TAPM concentrations. For odour impact and assessment, time series of short-term concentration variations, e.g. those over 1-minute intervals caused by plume meander, are required for a realistic quantitative analysis of the frequency and intensity of events. Presently TAPM, and most other models, are not capable of describing such time series in a physically realistic way.

7. Summary and conclusions

The work presented in this report is part of a study entitled "Meteorological and Dispersion Modelling Using TAPM for Wagerup", addressing three closely defined objectives. This report deals with the second objective (Phase 2: Dispersion), which was to:

- evaluate CSIRO's The Air Pollution Model (TAPM) for air quality predictions at Wagerup using a database of emissions from the Wagerup Refinery to model hourly-averaged ambient air concentrations of pollutants for appropriate periods and compare them with observations, and

- identify dominant pathways for the transport of the refinery emissions to the ground level in the surrounding district.

Results from Phase 1 (Meteorology), Phase 3A (TAPM modelling for Health Risk Assessment – Current Emission Scenarios) and Phase 3B (TAPM modelling for Health Risk Assessment – Expanded Refinery Scenario) are reported in the CSIRO (2004a), CSIRO (2004b) and CSIRO (2004c) reports, respectively.

TAPM is a prognostic meteorological and air pollution dispersion model developed by CSIRO Atmospheric Research (see http://www.dar.csiro.au/tapm). The meteorological component of TAPM predicts the local-scale flow, such as sea breezes and terrain-induced circulations, given the larger-scale synoptic meteorology. The air pollution component uses the model-predicted meteorology to estimate the pollutant concentrations in the region surrounding the emission source.

The specific components of the Phase 2 objective included:

- An analysis of the oxides of nitrogen (NO_x) data from Alcoa's Upper Dam and Boundary Road monitoring stations measured for a one-year period (1 April 2003–31 March 2004; the NO_x data at Upper Dam were available only till 12 December 2003), and an analysis of ANSTO perfluorocarbon tracer data obtained on 13 and 14 August 2002.

- Running TAPM for NO_x and ANSTO tracer data simulations, analysis of the model results, and comparison of the hourly-averaged model results with the data.

- For some periods, running of TAPM with building effects and local wind data assimilation.

- Calculation of a standard set of performance statistics for the model runs so that the performance of TAPM in estimating concentrations of air pollutants from given emissions can easily be compared with other models.

- An analysis of the total suspended particulate (TSP) data measured at the Residue Disposal Area (RDA) obtained for one year, and comparison of the model winds with the observed RDA winds when high TSP concentrations are observed.

- Identification of dominant meteorological and dispersion mechanisms governing the relative frequency of model events in the Yarloop area.

Information on the Refinery NO_x sources and their emission rates (constant with time), and tracer source characteristics was supplied by Alcoa. Alcoa also supplied the observed ambient concentrations of NO_x, total suspended particles, and ANSTO tracers.

In order to evaluate TAPM (version 2.6), it was run with four nested grid domains, with the innermost grid resolution of 0.5 km for meteorology and 0.25 km for dispersion. For pollutant dispersion, the innermost domain was about 7 km × 7 km, whereas the outermost domain was about 300 km × 300 km. Model inputs included the Wagerup-specific land-use database derived as part of the Phase 1 work.

The model evaluation focused on the ability of the model to describe the high concentration occurrences that are observed occasionally during the year and which are of most interest in impact assessments. For air pollution model evaluation, specific statistics are commonly used, including quantile-quantile (q-q) plots, and statistical measures, such as the robust highest concentration (RHC), and these were used in this study. The evaluation procedure involved comparison of modelled and observed concentrations that were unpaired in time and/or space.

The results of the Phase 2 are in summary:

- There is evidence that almost all of the Boundary Road NO_x data are heavily influenced by unquantified non-Refinery emissions, which are not included in the modelling, whereas the NO_x data from Upper Dam are the most extensive data set of measurements available that show a strong Refinery signature. Consequently, the emphasis was placed on the model comparison with the Upper Dam data for assessing the TAPM performance.

- The TAPM modelling performs well at Upper Dam. Considering all the statistical measures for high-end concentration (i.e. the maximum 1-hour average to the 99^{th} percentile), the ratio of the modelled concentration (with a background concentration added) to the observed one lies within 0.9–1.3. The model-observation comparison agrees to within the uncertainties in the model physics, inputs and concentration data.

- Inclusion of building wake effects in the model does not make a significant difference to the predictions. However, it is physically realistic to include them.

- Slight improvement in the TAPM predictions is achieved with the inclusion of the Refinery-generated heat flux.

- TAPM evaluation using a limited number of data from the ANSTO study indicates that without wind assimilation there is a bias in the model to underpredict the high-end concentration levels due to the 100-m Multiflue by a factor of about 2. For Calciner 4 and Boiler 1, the model performance is somewhat better, with some bias towards overprediction. With wind assimilation, the model performance improves substantially for the 100-m Multiflue. However, the model overpredicts the Calciner 4 and Boiler 1 concentrations to an even greater degree than without wind data assimilation.

- Wind data assimilation has mixed impact on pollution predictions. The results for NO_x at Upper Dam show that the assimilation of local wind data in TAPM makes

the modelled concentrations somewhat higher, and slightly improves the prediction of the top few concentrations that occur during the year. The ANSTO tracer-modelling results show that for Calciner 4 and Boiler 1, the wind data assimilation worsens the predictions, and for the 100-m Multiflue it improves the predictions.

- Meteorological data currently available for wind data assimilation do not cover the whole model year, and at the Residual Disposal Area have quality problems. More meteorological and pollution observations would be necessary to examine the impact of wind data assimilation on predictions within the larger, topographically complex domain of interest.

- The ability of TAPM to describe the winds measured at the RDA on occasions when elevated dust (defined as TSP) concentrations are observed in areas around the RDA for the period 1 April 2003–31 March 2004 was tested. The TSP concentrations show an increase with wind speed when it is above 7 m s-1. TAPM predicted the observed high wind speeds moderately well, with a correlation coefficient (r) between 0.6–0.7.

- Comparison of evaluation results reported in the present study with other modelling studies suggests that TAPM's overall performance at Wagerup is on par with its performance elsewhere for annual data measured at sparse monitoring networks. At Wagerup, some uncertainty in the model evaluation is generated by possible (unquantified) NO_x contributions from sources other than the Refinery.

- Using odour as a tracer, TAPM was run for the one-year period to identify meteorological and dispersion factors governing model events in Yarloop. A model event was defined as an occurrence when the model hourly average concentration exceeds a threshold level of 0.1 OU. The diurnal variation of the relative number (or the relative frequency) of model events qualitatively agrees with that of the relative number of complaints in the area.

- The maximum number (13%) of model events occur in the later morning, which closely matches the maximum number of complaints (15%) that occur at about the same time. Model events are most intense in the late morning when the airflow is such that Yarloop is frequently downwind of the Refinery.

- It is estimated that about 77% of the model events at Yarloop due to the Refinery emissions occur for model wind direction between 330°–60° when the Yarloop area is downwind of the Refinery. These events are dominated by morning inversion break-up fumigation, shallow convective mixing, and strong winds and/or cloudy conditions. About 15% of the model events that occur for model wind direction between 60°–150° are dominated by wind shear and nocturnal drainage flows from the escarpment with westerly flows aloft, while 8% of the model events that occur for model wind direction between 240°–330° are dominated by low/calm wind speed conditions.

- In terms of the meteorological variables that are used in routine modelling applications, the highest frequencies of model events are encountered when Yarloop is directly downwind of the Refinery; surface wind speed is moderately strong

(~2–6 m s^{-1}); atmospheric stability is neutral, slightly unstable or moderately unstable; and the boundary-layer height is less than 400 m.

Additional conclusions from Appendix A

The NO_x emissions initially supplied by Alcoa and used in model verification work presented in this report were constant throughout the annual model simulation period. Subsequent to the completion of the NO_x modelling, Alcoa supplied sufficient data on the daily operating conditions of Refinery processes and associated NO_x emissions to enable daily NO_x emission rates to be calculated. The Appendix A of this report presents the revised modelled ground-level concentrations based on these daily emission rates. The new results show that the approach of combining the buoyancies of the plumes from the Calciners 1–3 flues and those from the Boilers 1–3 flues, and treating them as effective single sources, produce better agreement between the modelled and observed NO_x concentrations at Upper Dam than when these flues are treated separately in the model (as was done in the report). For all the high-end concentration measures (i.e. the maximum 1-hour average to the 99^{th} percentile) at this site, the ratio of the modelled concentration (with a background concentration added) to the observed one ranged between 0.8–1.0. It is concluded that the observations support the use of plume buoyancy enhancement for modelling the emissions from the two Multiflue stacks of the Wagerup Refinery.

References

Alcoa: 2003. VOC Emission Rates – Post July 2002; Odour Emission Rates; SO_2 Emission Rates; Particulate Emission Rates [VOC etc Emission Rates.doc electronic document] Email to CSIRO Atmospheric Research from Patrick Coffey 7 April 2003. Australia: Alcoa World Alumina; 24 March 2003, 2 pp.

ASTM: 2000. Standard guide for statistical evaluation of atmospheric dispersion model performance, Designation: D 6589 – 00, American Society for Testing and Materials, West Conshohocken, PA, 17 pp.

Cox, W. M., Tikvart, J. A.: 1990. A statistical procedure for determining the best performing air quality simulation model. *Atmospheric Environment* **24A**, 2387–2395.

CSIRO: 2004a. Meteorological and Dispersion Modelling Using TAPM for Wagerup: Phase 1: Meteorology, Report to Alcoa World Alumina Australia, February 2005, 103 pp.

CSIRO: 2004b. Meteorological and Dispersion Modelling Using TAPM for Wagerup: Phase 3A: HRA (Health Risk Assessment) Concentration Modelling – Current Emission Scenarios, draft report to Alcoa World Alumina Australia, November 2004, 43 pp.

CSIRO: 2004c. Meteorological and Dispersion Modelling Using TAPM for Wagerup: Phase 3B: HRA (Health Risk Assessment) Concentration Modelling – Expanded Refinery Scenario, draft report to Alcoa World Alumina Australia, February 2005, 133 pp.

CSIRO: 2004d. Wagerup Air Quality Review, Report to Alcoa World Alumina Australia, May 2004, 133 pp.

Dabberdt, W. F., Dietz, R. N.: 1986. Gaseous tracer technology and applications. In: *Probing the Atmospheric Boundary Layer* (editor D. H. Lenschow), American Meteorological Society, Boston, pages 103–128.

EPAV: 2000. AUSPLUME Gaussian Plume Dispersion Model: Technical User Manual, Environment Protection Authority of Victoria, Australia, http://www.epa.vic.gov.au.

Galbally, I. E., Freney, J. R., Muirhead, W. A., Simpson, J. R. Trevitt, A. C. F., Chalk, P. M.: 1987. Emission of nitrogen oxides (NO_x) from a flooded soil fertilized with urea: relation to other nitrogen loss processes. *Journal of Atmospheric Chemistry* **5**, 343–365.

Hanna, S.R.: 1988. Air quality model evaluation and uncertainty. *Journal of Air Pollution Control Association* **38**, 406–412.

Hurley, P. J.: 2002, The Air Pollution Model (TAPM) Version 2. Part 1: Technical Description, CSIRO Atmospheric Research Technical Paper No. 55. Available at http://www.dar.csiro.au/TAPM.

Hurley, P. J., Blockley, A., Rayner, K.: 2001. Verification of a prognostic meteorological and air pollution model for year-long predictions in the Kwinana region of Western Australia. *Atmospheric Environment* **35**, 1871–1880.

Hurley, P. J., Luhar, A. K.: 2005. An evaluation and inter-comparison of AUSPLUME, CALPUFF and TAPM. Part I: the Kincaid and Indianapolis field datasets. *Clean Air and Environmental Quality (Aust.)* **39** (1), February 2005.

Hurley, P. J., Physick, W. L., Luhar, A. K.: 2002. The Air Pollution Model (TAPM) Version 2. Part 2: Summary of some verification studies, CSIRO Atmospheric Research Technical Paper No. 57. 46 pp.

Hurley, P., Manins, P., Lee, S., Boyle, R., Ng, Y. L., Dewundege, P.: 2003. Year-long, hi-resolution, urban airshed modelling: verification of TAPM predictions of smog and particles in Melbourne, Australia. *Atmospheric Environment* **37**, 1899–1910.

Luhar, A. K.: 2002. The influence of vertical wind direction shear on dispersion in the convective boundary layer, and its incorporation in coastal fumigation models. *Boundary-Layer Meteorology* **102**, 1–38.

Luhar, A. K., Hurley, P. J.: 2003. Evaluation of TAPM, a prognostic meteorological and air pollution model, using urban and rural point-source data. *Atmospheric Environment* **37**, 2795–2810.

Physick, W.L., Blockley, A.: 2001. An evaluation of air quality models for the Pilbara region, CSIRO Division of Atmospheric Research. A Report to the Department of Environmental Protection, Western Australia, 98 pp, June 2001.

Physick, W. L., Blockley, A., Farrar, D., Rayner, K., Mountford, P.: 2002. Application of three air quality models in the Pilbara region, *Proceedings of the 16th International Clean Air and Environment Conference*, Christchurch, New Zealand, August 2002.

Rayner, K. N.: 1987. Dispersion of atmospheric pollutants from point sources in a coastal environment. Ph.D. thesis, Murdoch University, Western Australia, 249 pp.

Rayner, K. N.: 1998. A model-based sulfur dioxide control policy for the Kwinana industrial region. *Proceedings of the 11th Clean Air and Environment Conference*, Durban, South Africa, 13–18 September.

Riley, G.: 2002. Odour statistics report: complaint vs complaint free data comparisons: hourly process & weather variables (Wagerup CCDB & ROT data: Dec 2001 - Nov 2002). Alcoa World Alumina Technology Delivery Group; December 2002. 22 p.

SKM: 2002. Wagerup Refinery Odour Assessment, Final report, Sinclair Knight Merz, February 2002.

SKM: 2003a. Alcoa of Australia Limited: Wagerup Tracer Modelling, Final report, Sinclair Knight Merz, July 2003.

SKM: 2003b. Alcoa World Alumina Australia: Wagerup weather station and ambient dust monitoring program review following implementation of audit findings. Sinclair Knight Merz, Bunbury, WA (Australia), 28 June 2004, pp. 27.

Venkatram, A., Brode, R., Cimorelli, A., Lee, R., Paine, R., Perry, S., Peters, W., Weil, J., Wilson, R.: 2001. A complex terrain dispersion model for regulatory applications. *Atmospheric Environment* **35**, 4211–4221.

Venkatram, A., Isakov, V., Yuan, J., Pankratz, D.: 2004. Modeling dispersion at distances of meters from urban sources. *Atmospheric Environment* **38**, 4633–4641.

Appendix A: Estimates of daily variation in NO_x emission rates and recalculation of the ground-level concentrations

In Section 4.2 of this report, the emission rates of NO_x used by TAPM for all stack sources considered were constant throughout the annual model simulation period (1 April 2003 – 31 March 2004). This was the information supplied by Alcoa at the time. Hence, there was no hourly, daily or seasonal variation of the NO_x emission rates included in the modelling. Subsequent to the completion of the NO_x modelling described in Section 4.2, Alcoa supplied sufficient data on the daily operating conditions of Refinery processes and associated NO_x emissions to enable daily NO_x emission rates to be calculated. This Appendix presents the revised modelled ground-level concentrations based on these daily emission rates and compares them with the available NO_x observations. Subsequently, the approach of combining the buoyancies of the plumes (called plume buoyancy enhancement) from the Multiflue stacks is discussed. Its use in the modelling is shown to produce good agreement between the modelled and observed NO_x concentrations, and it is concluded that plume buoyancy enhancement is the appropriate choice for modelling the emissions from the two Multiflue stacks of the Wagerup Refinery.

A.1 Estimation of daily variation in NO_x emission rates

The subsequent analysis is based on the fact that NO_x emissions from most sources have a definite relationship with the operating conditions of the source. The procedure for estimating the daily variation in NO_x emission rates involves two main steps: 1) determine a relation between operating conditions and NO_x emission rates for each of the nine NO_x sources (i.e. Liquor Burner, Calciners 1–4, Boilers 1–3, and Gas Turbine), and 2) use these relations with data on the daily operating conditions to compute daily average NO_x emission rate for each source.

Alcoa provided results from a NO_x monitoring study, in which NO_x emission rates were measured as a function of operating conditions, in the electronic data file "2002-03 Calciner and boiler NO_x investigation v2.xls". Alcoa provided details of daily operating process variables in the files "Combustion source process variables Boilers HRSG & LB 2003 to Q3 2004.xls", and "Combustion source process variables CALCINERS 2002 to Q3 2004.xls".

A.1.1 Relation between operating conditions and NO_x emission rates

For most sources, data were available from a set of NO_x investigations for loads between 50% and 100%. For the Calciners 1–4, Boilers 1–3 there are data on the NO_x emission rates corresponding to selected Natural Gas Consumption (GC) Rates for each source in the file "2002-03 Calciner and boiler NOx investigation v2.xls". These data are plotted as the diamonds in the following Figures A1 (a–g) corresponding to these seven NO_x sources. A linear fit (solid line) is made to these data points with the regression equation(s) given on each figure. For GC rates below the lowest data point, a linear extrapolation to zero (dotted line) was used to represent emission rates for operation in this region. For the Gas Turbine, shown in Figure A1 (h) the operating variable that relates to NO_x emissions is Gas Turbine Load (Power Recovery %).

The filled area shows the frequency distribution of the natural gas consumption rate in Figures A1 (a–g) and load for the Gas Turbine in Figure A1 (h) for the year of interest

(1 April 2003 to 31 March 2004). It is seen that the data used to obtain the regression match the main operating conditions quite well, giving confidence to the use of the regressions for computing the daily NO_x emission rates.

For Boiler 1 (Figure A1 (a)), linear fits covering two separate ranges were made to match the data as closely as possible because of the significance of the Boiler 1 emissions (typically 30% of the total NO_x emissions).

For the Gas Turbine (GT), Alcoa recommends that it is better to use load rather than gas consumption rate for the analysis. The load for the GT is defined as percent GT power recovery. Each of the ten burners of the GT combustion system has a primary and a secondary zone. At various loads, the combustion efficiency and gas flow rates vary between the primary and secondary regions. Between approximately 65 % and 75% GT load, the burner configuration changes to pre-mix mode, in which fuel is added to both the primary and secondary zones, but combustion only occurs in the secondary zone. In the primary zone, air and fuel are mixed and pass into the secondary zone before being combusted. Premixing the air and fuel reduces gas turbine exhaust NOx emissions (Alcoa, 2004). Figure A1 (h) shows the two operating regimes of the Gas Turbine. The first is at low loads (up to 75% load) where NO_x emissions increase with load. The other is at high loads (above 75% load) where the premixing the air and fuel is used that gives low NO_x production so that NO_x emissions are much lower and may be considered approximately independent of load. Figure A1 (h) shows separate fits for each of these regions. For comparison, the fits reported in the Alcoa "Nitrogen Oxides (NO_x) and Carbon Monoxide (CO) Monitoring Program Report" (Alcoa, 2004) are included. The agreement at low loads is very good. At high loads, the Alcoa fits shows a dependence on load. As the final results for NO_x emissions are not very sensitive to the fit in this region, the constant emission rate of 16 kg/hr was used to maintain consistency with the approach used for determining the NO_x vs. Gas Consumption correlations in the rest of the analysis presented here.

For the Liquor Burner, Alcoa has reported that there is no correlation between NO_x emission rates and dryer feed rate or kiln pressure, so that the results from each of the tests reported in the file "2002-03 Calciner and boiler NO_x investigation v2.xls" are plotted against test number (see Figure A1 (i)). On the left-hand side of Figure A1 (i), the approximately normal (Gaussian) distribution of NO_x emission rates presented in the Alcoa (2004) report has been replotted in units of kg/hr. There is reasonable agreement between the average of the data (diamonds) (2.3 kg/hr) and the mean of the Gaussian distribution. As there is no information available to determine the daily variation in the Liquor Burner NO_x emissions and the average is only about 2% of the total Refinery emissions, the assumption of constant emission rates is reasonable for the purposes of this analysis.

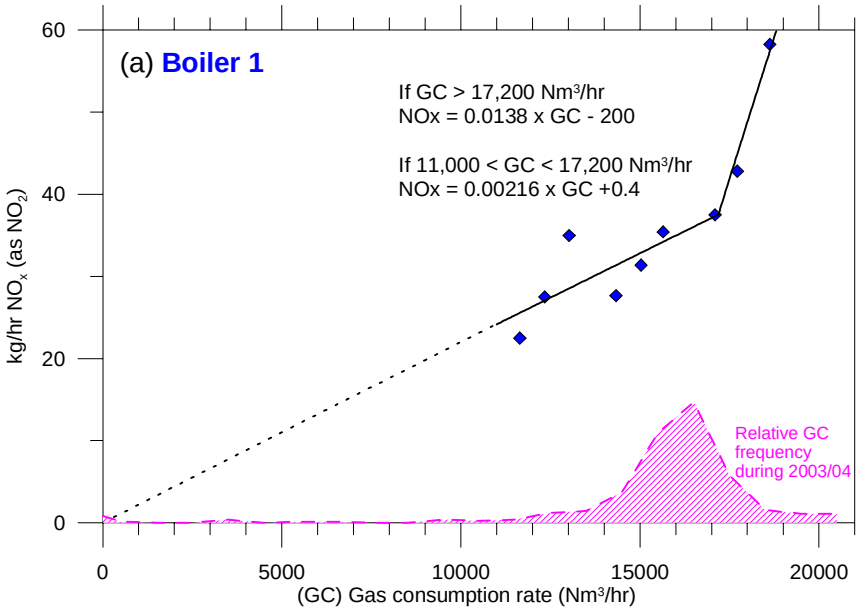

Figure A1 (a): Variation of the measured NO_x emission rate with the natural gas consumption (GC) rate (diamonds) for Boiler 1. The solid lines are fits to the data. The relative frequency distribution of the gas consumption rate is shown by the filled area.

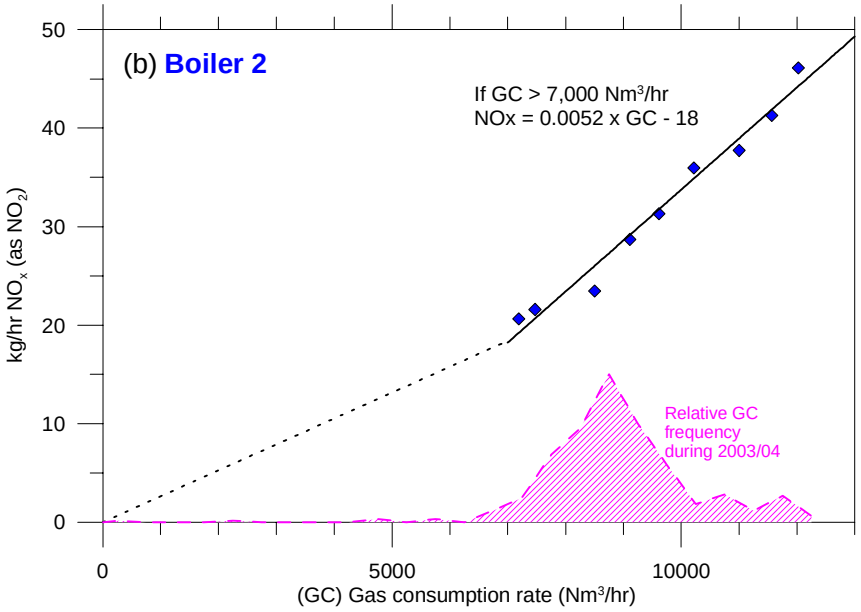

Figure A1 (b): Variation of the measured NO_x emission rate with the natural gas consumption (GC) rate (diamonds) for Boiler 2. The solid line is a fit to the data. The relative frequency distribution of the gas consumption rate is shown by the filled area.

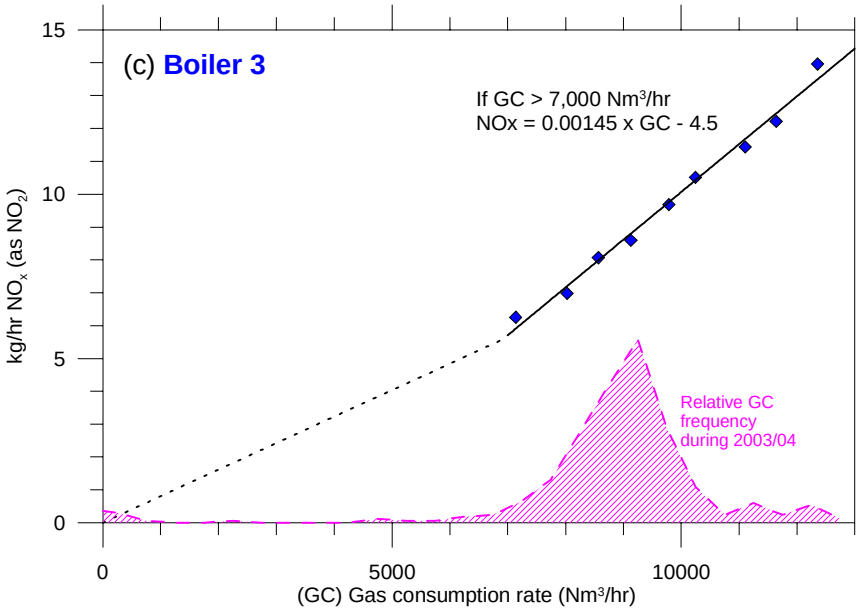

Figure A1 (c): Variation of the measured NO_x emission rate with the natural gas consumption (GC) rate (diamonds) for Boiler 3. The solid line is a fit to the data. The relative frequency distribution of the gas consumption rate is shown by the filled area.

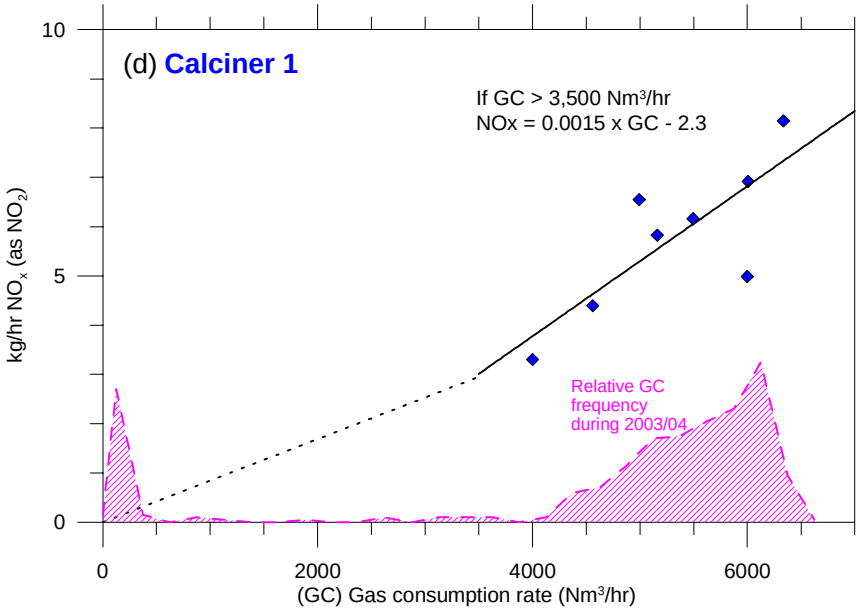

Figure A1 (d): Variation of the measured NO_x emission rate with the natural gas consumption (GC) rate (diamonds) for Calciner 1. The solid line is a fit to the data. The relative frequency distribution of the gas consumption rate is shown by the filled area.

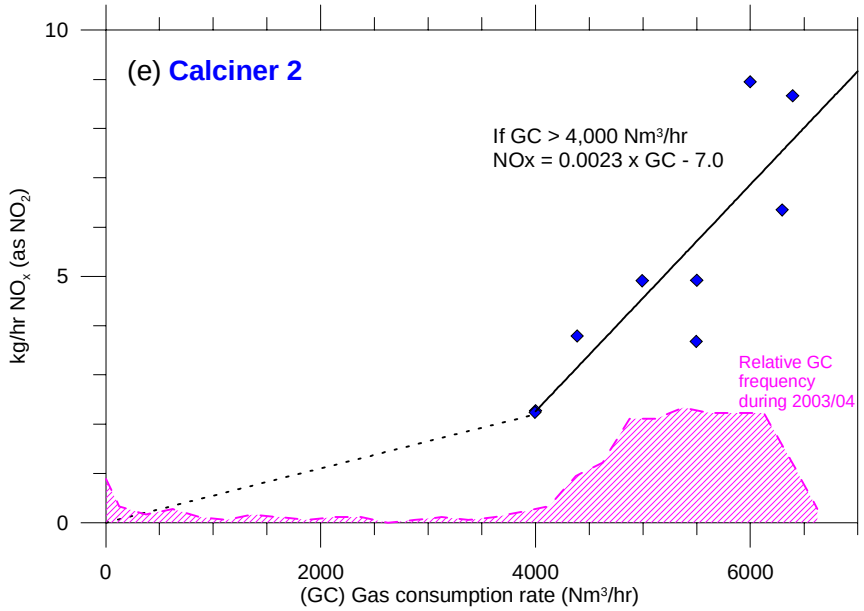

Figure A1 (e): Variation of the measured NO_x emission rate with the natural gas consumption (GC) rate (diamonds) for Calciner 2. The solid line is a fit to the data. The relative frequency distribution of the gas consumption rate is shown by the filled area.

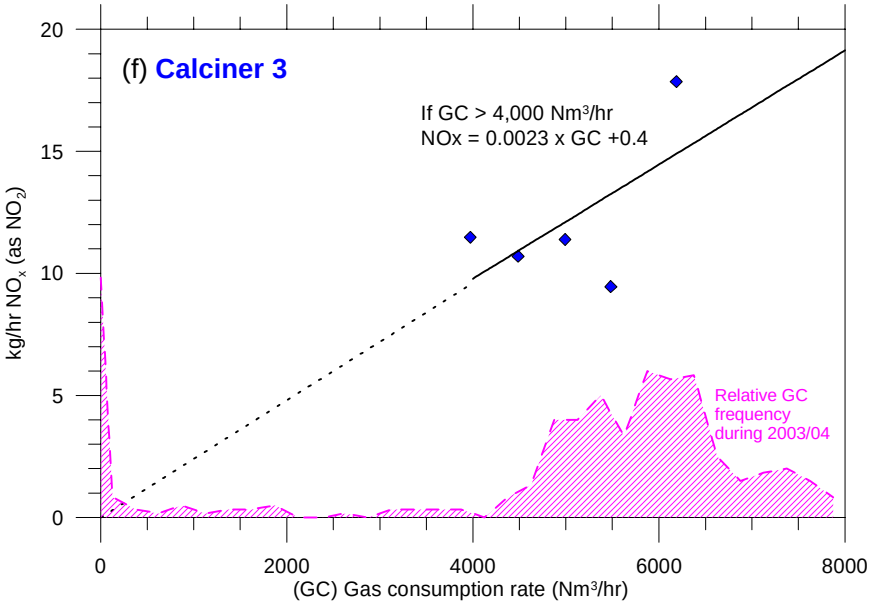

Figure A1 (f): Variation of the measured NO_x emission rate with the natural gas consumption (GC) rate (diamonds) for Calciner 3. The solid line is a fit to the data. The relative frequency distribution of the gas consumption rate is shown by the filled area.

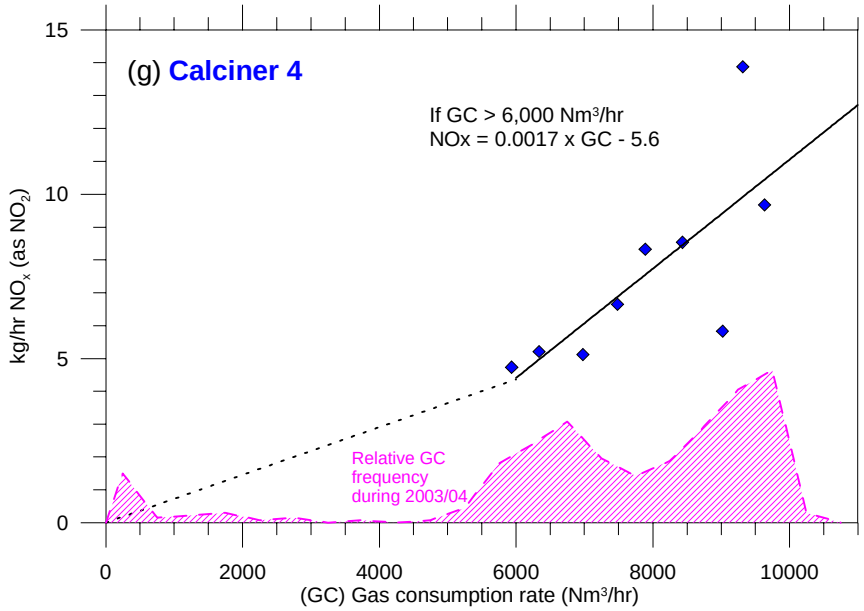

Figure A1 (g): Variation of the measured NO_x emission rate with the natural gas consumption (GC) rate (diamonds) for Calciner 4. The solid line is a fit to the data. The relative frequency distribution of the gas consumption rate is shown by the filled area.

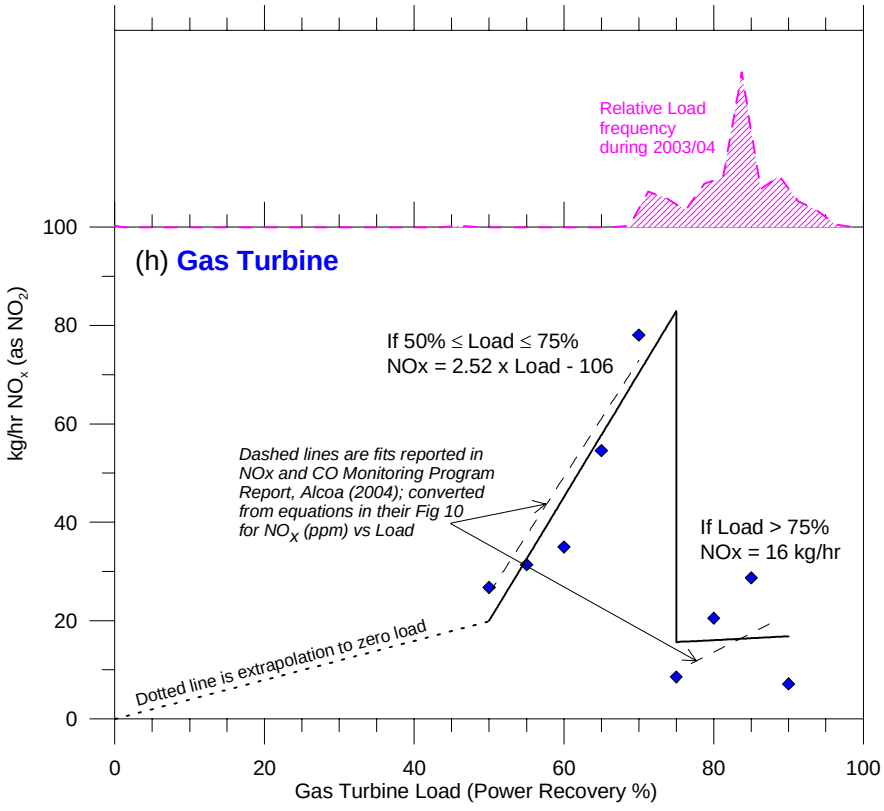

Figure A1 (h): Variation of the measured NO_x emission rate with the load (diamonds) for Gas Turbine. The solid lines are fits to the data. The relative frequency distribution of the gas consumption rate is shown by the filled area (top figure).

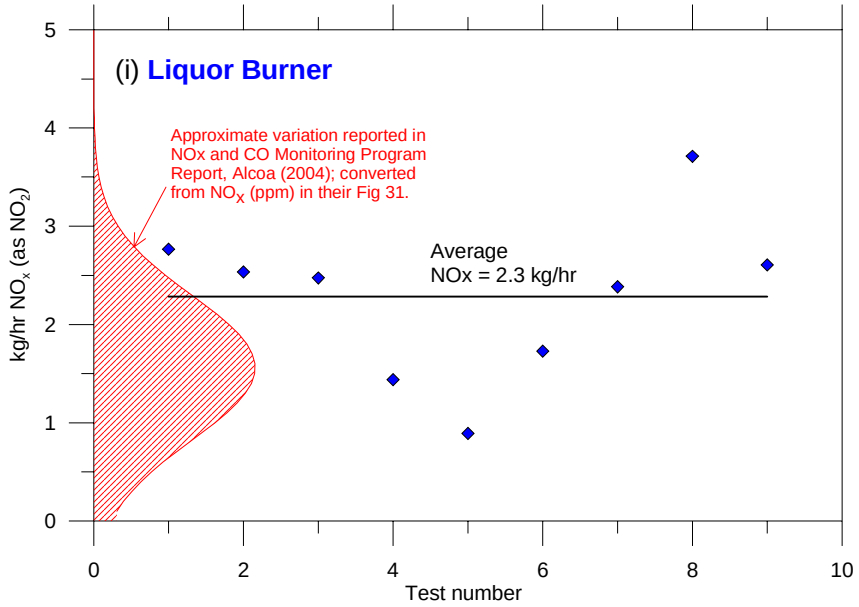

Figure A1 (i): Variation of the measured NOx emission rate with as a function of the test number (diamonds) for Liquor Burner (see text for details).

A.1.2 Computing daily NO_x emission rate for each source

The daily natural gas consumption rates (or the load for the Gas Turbine) provided by Alcoa were used, together with the regression relationships presented above, to compute the daily average NO_x emission rates from each source. The results in the following Figure A2 (a–i) show the daily variation in the total NO_x emissions from the nine sources at the Wagerup Refinery for the year 1 April 2003 – 31 March 2004. Figure A2 (j) shows this variation for all the sources combined.

The total annual average NO_x emission rate is computed to be 35.4 g/s and the annual median is 33.5 g/s. There is a significant period during September to November when the total daily average emission rate is between 45 and 55 g/s. The constant total NO_x emission rate previously provided by Alcoa, reported in Table 1 of the present report, is 31.9 g/s. In the Phase 3 report, modelling is undertaken using an average NO_x emission rate of 31.9 g/s and a peak emission rate of 75.2 g/s for the Current Refinery Scenarios.

In the next Section, these daily NO_x emission rates are used to revise the modelled NO_x ground-level concentrations reported in Section 4.2.

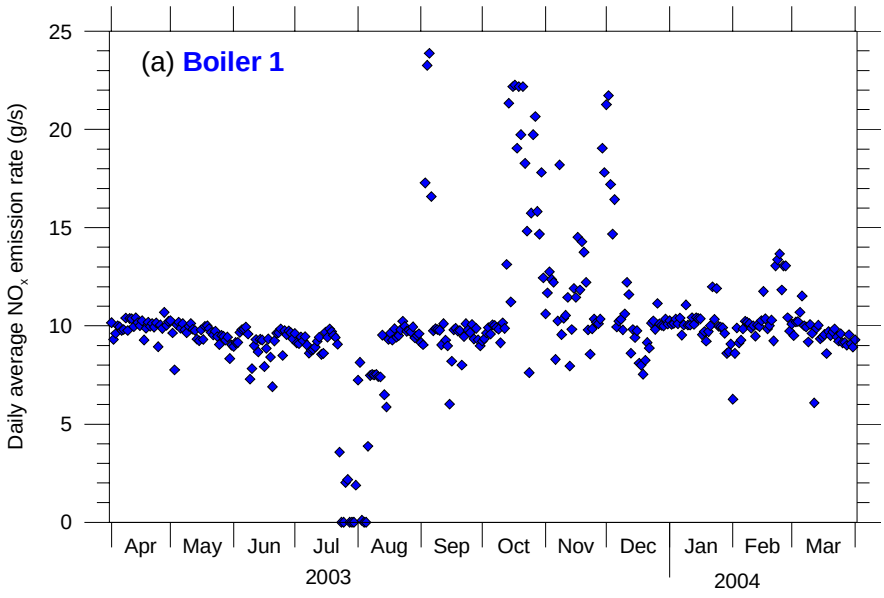

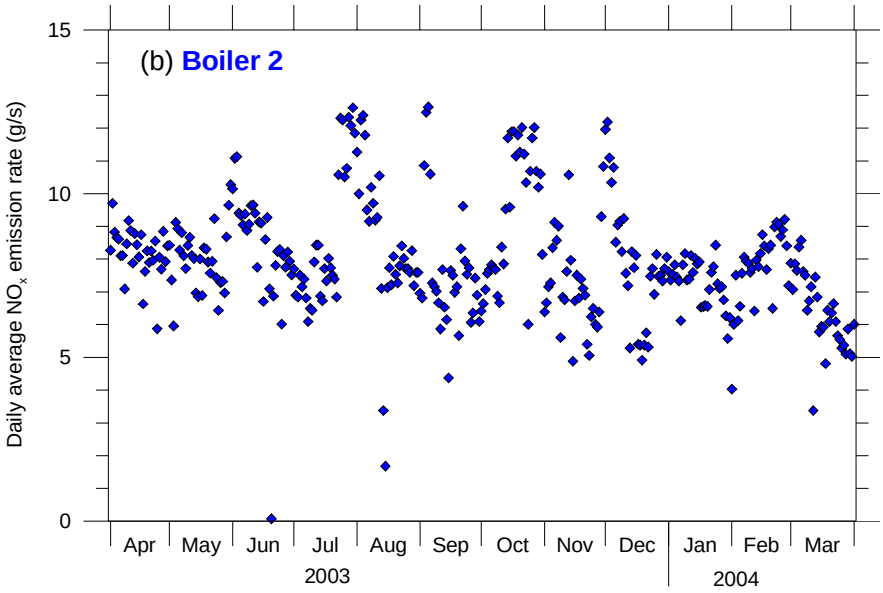
(b) Boiler 2
Daily average NOx emission rate (g/s)
15
10
5
0
Apr
May
Jun
Jul
Aug
Sep
Oct
Nov
Dec
Jan
Feb
Mar
2003
2004

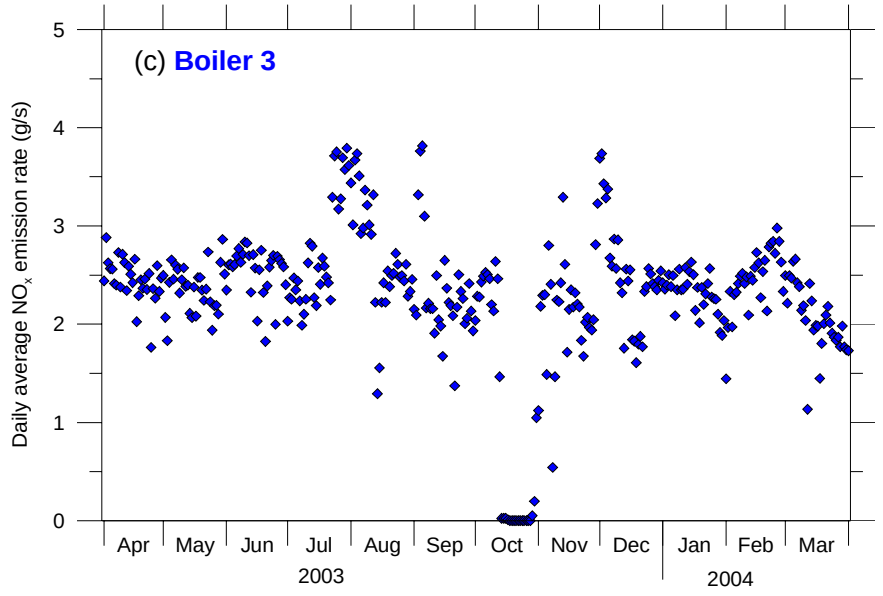
(c) Boiler 3
Daily average NOx emission rate (g/s)
5
4
3
2
1
0
Apr
May
Jun
Jul
Aug
Sep
Oct
Nov
Dec
Jan
Feb
Mar
2003
2004

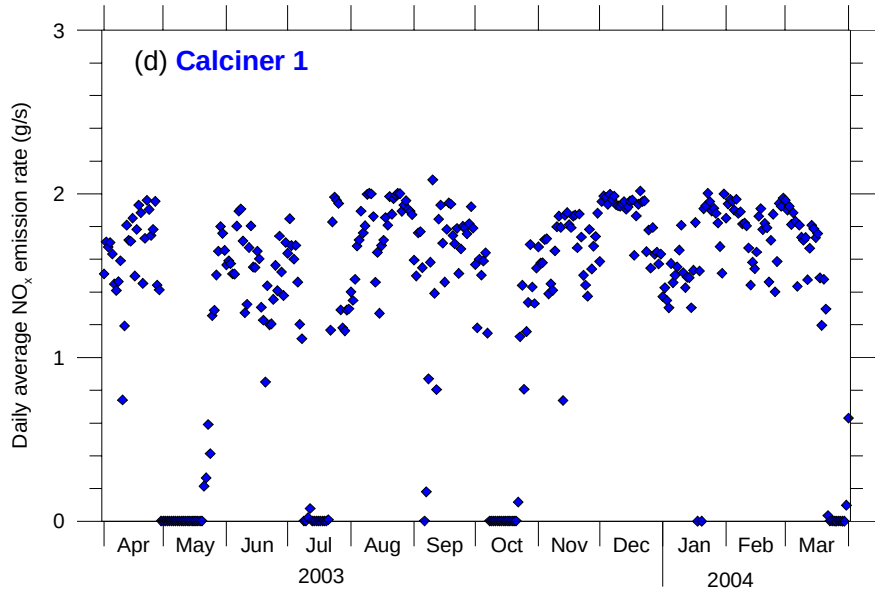
(d) Calciner 1
Daily average NOx emission rate (g/s)
3
2
1
0
Apr
May
Jun
Jul
Aug
Sep
Oct
Nov
Dec
Jan
Feb
Mar
2003
2004

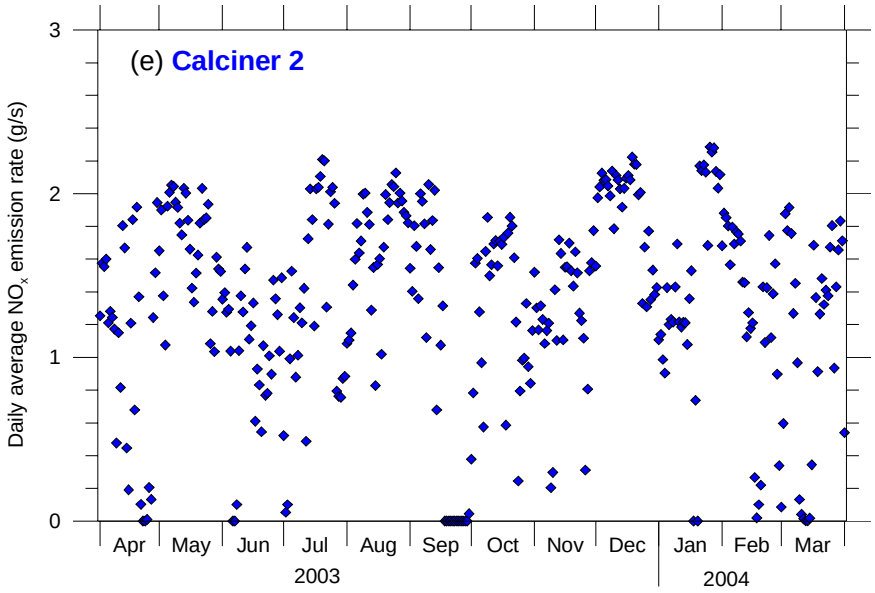
(e) Calciner 2
Daily average NOx emission rate (g/s)
0
1
2
3
Apr
May
Jun
Jul
Aug
Sep
Oct
Nov
Dec
Jan
Feb
Mar
2003
2004

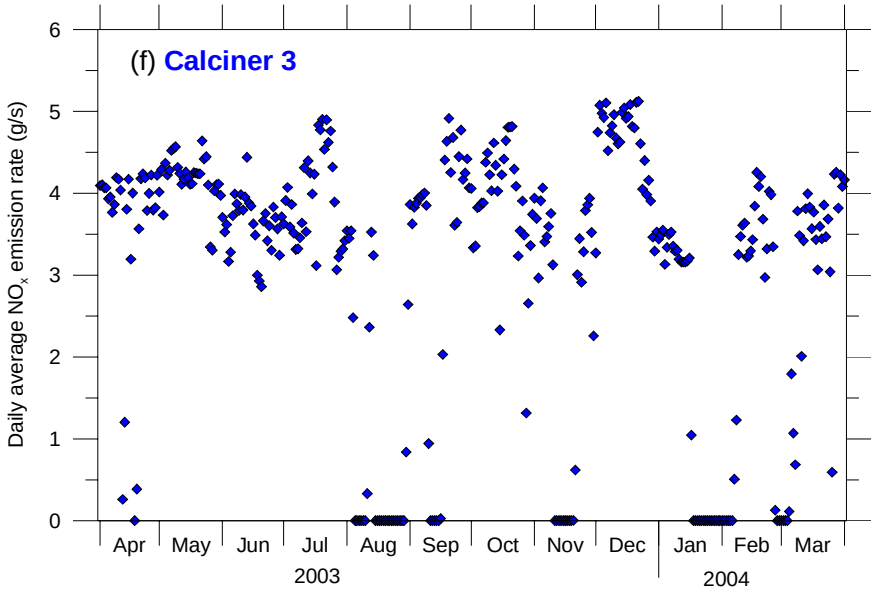
(f) Calciner 3
Daily average NOx emission rate (g/s)
0
1
2
3
4
5
6
Apr
May
Jun
Jul
Aug
Sep
Oct
Nov
Dec
Jan
Feb
Mar
2003
2004

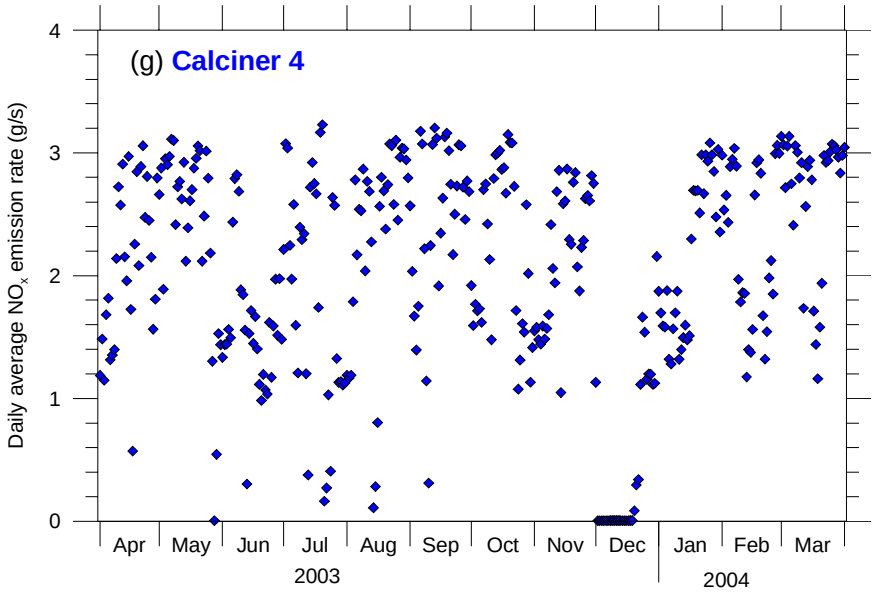
(g) Calciner 4
Daily average NOx emission rate (g/s)
0
1
2
3
4
Apr
May
Jun
Jul
Aug
Sep
Oct
Nov
Dec
Jan
Feb
Mar
2003
2004

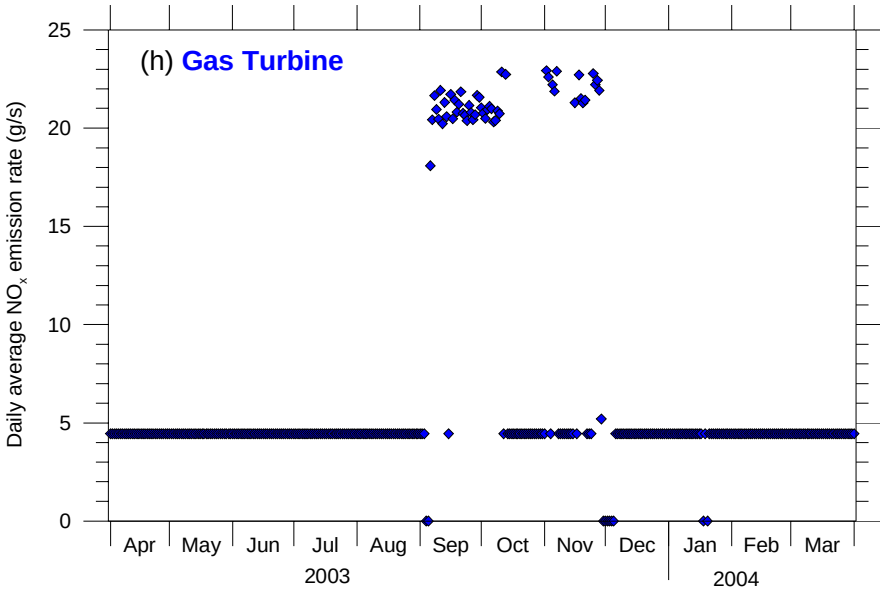
(h) Gas Turbine
Daily average NOx emission rate (g/s)
25
20
15
10
5
0
Apr
May
Jun
Jul
Aug
Sep
Oct
Nov
Dec
Jan
Feb
Mar
2003
2004

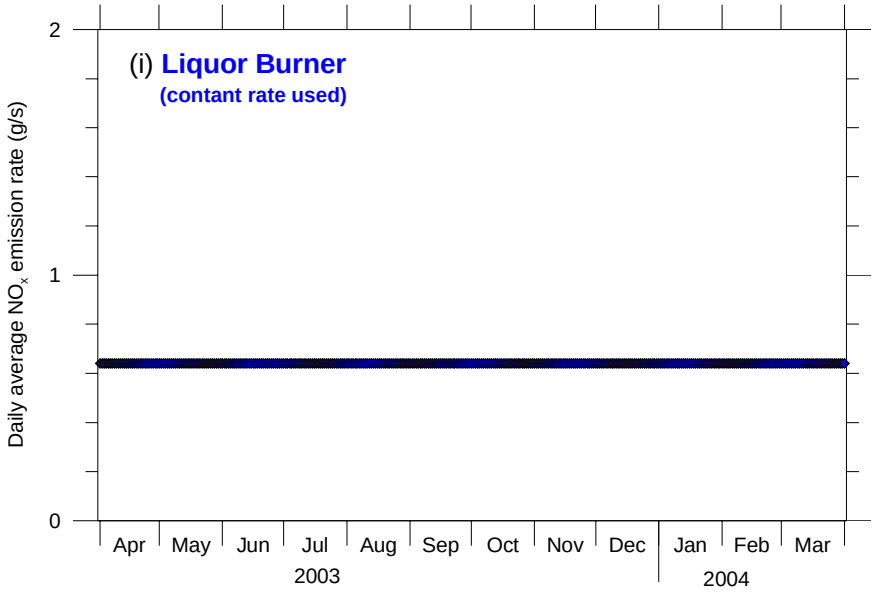
(i) Liquor Burner
(contant rate used)
Daily average NOx emission rate (g/s)
2
1
0
Apr
May
Jun
Jul
Aug
Sep
Oct
Nov
Dec
Jan
Feb
Mar
2003
2004

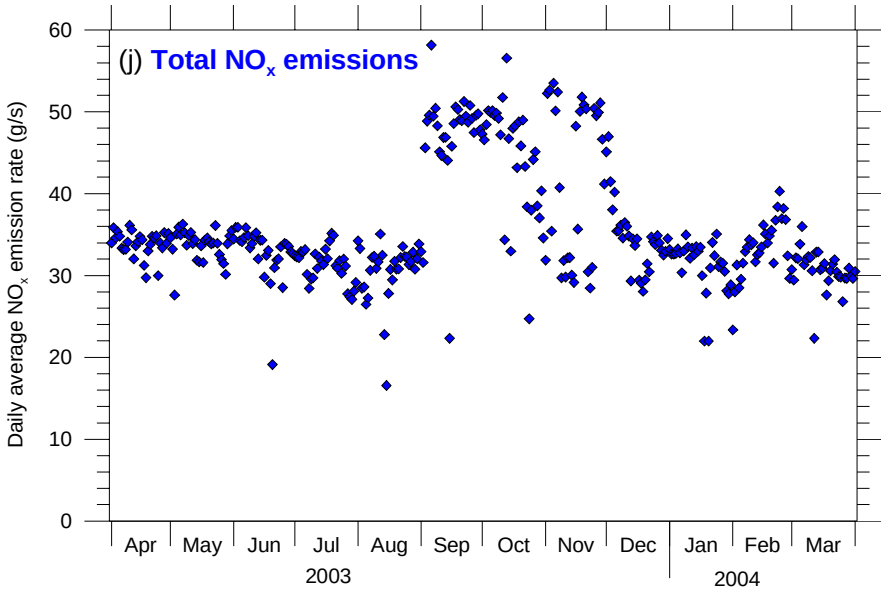

Figure A2: Time series of the computed daily NO_x emission rate for (a) Boiler 1, (b) Boiler 2, (c) Boiler 3, (d) Calciner 1, (e) Calciner 2, (f) Calciner 3, (g) Calciner 4, (h) Gas Turbine, and (i) Liquor Burner. The time series of the total daily NO_x emission rate is shown in figure (j).

A.2 Recalculation of the modelled ground-level NO_x concentrations

In Section 4.2, TAPM modelling results for NO_x were presented and compared with available NO_x observations at Upper Dam and Boundary Road. The Boundary Dam data were identified as not as robust as the Upper Dam data because of the contributions to the former by non-Refinery sources not included in the modelling. This is further supported by the data plotted in Figure A3 and Figure A4.

Figure A3 shows a scatter plot of the observed 6-minute NO_x concentration at Upper Dam vs. the observed 6-minute NO_x concentration at Boundary Road when the observed wind direction is from the sector 180°–240° (i.e. Upper Dam is downwind and Boundary Road is upwind of the Refinery). The 6-minute wind direction observations taken at 10-m AGL during 1 April–18 July 2003 and those taken at 30-m AGL during 18 July 2003–31 March 2004, at Bancell Road were used for filtering the data. The main point to note in Figure 3A is that there is a well-defined Refinery signal at Upper Dam, with the corresponding NO_x levels at Boundary Road generally being much lower. There are a very few cases in which the concentrations at Boundary Road are higher than those at Upper Dam, even though the former is upwind of the Refinery. This most probably is due to non-Refinery sources affecting NO_x levels at Boundary Road.

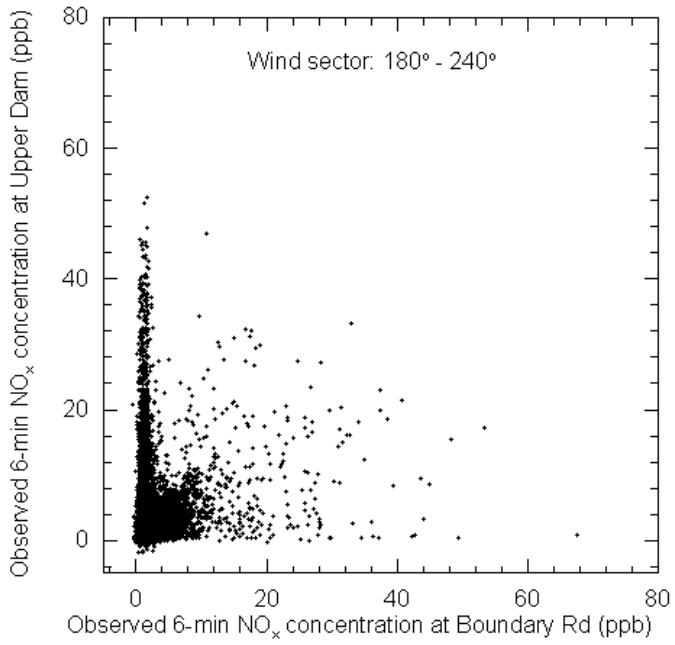

Figure A3: Scatter plot of the observed 6-minute NO_x concentration at Upper Dam vs. the observed 6-minute NO_x concentration at Boundary Road when the observed wind direction is from the sector 180°–240°.

In Figure A4, the observed 6-minute NO_x concentration at Boundary Road are plotted against the observed 6-minute NO_x concentration at Upper Dam when the observed wind direction is from the sector 330°–60° (i.e. Boundary Road is downwind and Upper Dam is upwind of the Refinery). It is clear from Figure A4 that, compare to Figure A3

for Upper Dam, there is not a dominant Refinery impact at Boundary Road. It appears that the relative contribution of non-Refinery/regional sources to the NO_x concentrations at Boundary Road is much larger than that at Upper Dam.

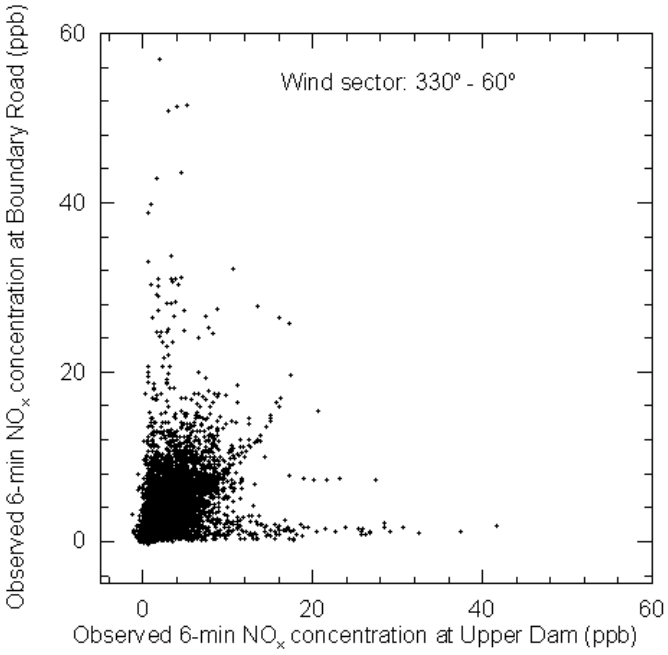

Figure A4: Scatter plot of the observed 6-minute NO_x concentration at Upper Dam vs. the observed 6-minute NO_x concentration at Boundary Road when the observed wind direction is from the sector 330°–60°.

The above analysis indicates that almost all of the Boundary Road data are heavily influenced by non-Refinery emissions. Consequently the Boundary Road data cannot be used for assessing the TAPM modelling because the modelling only included Refinery sources of NO_x.

The modelling in Section 4.2 used a constant total NO_x emission rate of 31.9 g/s (the best data available at the time). The quantile-quantile (q-q) plot in Figure 8 showed good agreement between the modelled and observed concentrations at Upper Dam for Run B (with building wake effects, no wind data assimilation) and with all the NO_x sources treated as separate sources, i.e. no plume interaction and hence no buoyancy enhancement of any of the plumes.

The new data on the daily variations in NO_x (Figure A2(j)) shows that the emission rates were actually significantly higher than 31.9 g/s during September to December so that TAPM results presented in Section 4.2 would have underestimated the ground-level concentrations.

Thus we used the new NO_x emission rates to scale the original TAPM predicted NO_x concentrations. (Ideally, when computing hourly-averaged concentrations, hourly-averaged emission rates should be used, but only daily-average emission rate are available.) The procedure adopted was to use each daily-average NO_x emission rate for scaling for each source for all hours of that day for that source. The scaled concentrations due to all sources at a given location were summed up to determine the total NO_x concentration at that location. A background NO_x concentration of 2 ppb, based on observations, was added to the modelled concentrations. No data were

provided on variability in the stack exit temperature and the stack exit velocity. Consequently this study assumed that these parameters are constant with the values given in Table 1.

With the new NO_x emission rates and the same other modelling set-up as previously used for Figure 8 (building wakes, no data assimilation, no buoyancy enhancement), TAPM overpredicts the NO_x concentrations at Upper Dam, as seen in Figure A5. The main reason for this overestimation is established to be the way the Refinery Multiflue sources are handled in the modelling. This is discussed below.

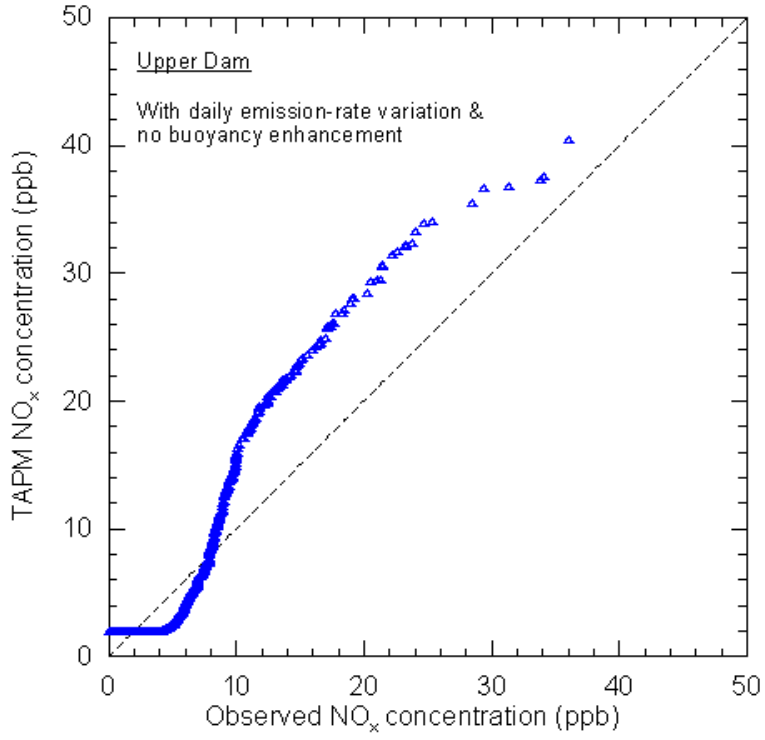

Figure A5: Quantile-quantile plots of the hourly-averaged modelled vs. observed NO_x concentrations for Upper Dam. The modelled concentrations were computed using the daily variation of the emission rates, with all multiflue stacks considered as separate stacks (i.e. no buoyancy enhancement).

A.2.1 Combining closely-spaced sources (buoyancy enhancement)

The 100-m Multiflue and the 65-m Boilers 1–3 Multiflue contain several closely-spaced flues which release buoyant plumes, i.e. the exit temperature of the gas emitted from the flue is greater than the temperature of the surrounding air. The Boiler Multiflue has three flues, each with a diameter of about 2 m, and with a separation between the flues of less than 3 m. Similarly, the 100-m multiflue stack consists of five stacks: Liquor Burner, Vacuum Pump, and Calciners 1–3; the first two with a diameter of about 1 m each and the three Calciners stacks with a diameter of about 2 m each. The separation between these five stacks is less than 5 m.

Buoyant plumes emitted from closely-spaced flues tend to merge quickly with one another after their release (Anfossi et al, 1978; Briggs, 1984; Overcamp and Ku, 1988; Manins et al, 1992; Konig and Mokhtarzadeh-Dehghan, 2002). This merging results in

an enhancement of the plume buoyancy, thus causing a greater plume rise of the combined plume than the individual plume rises that occur when the flues are treated as separate point sources. The enhancement of the plume buoyancy (and plume rise) can be understood by noting that as the hot air rises it mixes in (entrains) cooler surrounding air, which reduces the temperature of the rising plume. Eventually the temperature of the air in the plume is reduced to that of the surrounding air and the plume stops rising. If one buoyant plume is rising close to another buoyant plume, then some of the air entrained by the first plume will be the warmer air from the second plume rather than the cooler surrounding air. This causes both plumes together to rise higher than they would individually.

In cases where each flue of a multiflue has the same emission geometry and exit conditions, then all such flues can be modelled as a combined source (single plume) that has its buoyancy flux (F_b) and momentum flux (F_m) equal to (or as close as possible to) the sum of these quantities for the individual flues. The pollution emission rate from the effective combined source is set equal to the sum of the pollution emission rates from the individual flues.

The quantities F_b ($m^4\ s^{-3}$) and F_m ($m^4\ s^{-2}$) are defined as:

$$F_b = \left(1 - \frac{T_e}{T_s}\right) g\, w_s\, r_s^2\,, \tag{A1}$$

$$F_m = \left(\frac{T_e}{T_s}\right) w_s^2\, r_s^2\,, \tag{A2}$$

where T_e is the ambient temperature (K) of the environment, T_s is the stack exit temperature (K), r_s is the stack top radius (m), w_s is the stack exit velocity ($m\ s^{-1}$), and g is the acceleration due to gravity ($m\ s^{-2}$).

A common method for matching the fluxes is first to set the diameter of the combined source such that the exit area of the combined source is equal to the sum of the areas of the flues being combined. Then the combined source exit velocity and exit temperature are set equal to the averages of the values for the individual flues. Small adjustments to the exit velocity and temperature are then be made to match the buoyancy and momentum fluxes of the combined source as closely as possible to the sums of these quantities for the individual flues. For cases where the buoyancy flux dominates the plume rise (such as for the Wagerup plumes), it is more important to match the buoyancy flux than the momentum flux.

Table 1 lists the properties of the individual stack sources included in the modelling. Based on the earlier discussion, we model the Calciner 1–3 flues and Boilers 1–3 flues as combined sources. The Liquor Burner flue and the Calciner 1–3 Vacuum Pump and Dorrco flue (not listed as a NO_x source) are part of the 100-m Multiflue with the Calciner 1–3 flues but the first two have not been included in the combined source because of their quite different emission characteristics (stack exit temperature and stack exit velocity), which lead to different plume trajectories.

The trajectory of a plume above its release point is given by the relation (Briggs, 1984):

$$z = \left(8.3\frac{F_m}{U^2}\cdot x + 4.2\frac{F_b}{U^3}\cdot x^2\right)^{\frac{1}{3}}, \tag{A3}$$

where z is the height of the plume above the release point, x is the downwind distance from the source, and U is the local wind speed at stack height.

The trajectories of the individual plumes from the 100-m Multiflue assuming no interaction between the plumes are shown in Figure A6 for a wind speed of 4 m s^{-1}. Changes in the wind speed change the absolute heights of the plume but not the relativities between the trajectories of the plumes from the different flues. The similarity of the plume rise from the three Calciner flues reflects the similarities between their emission characteristics and justifies them being treated as a combined source. As expected and shown in Figure A6, the trajectory for the combined source of the three Calciner flues shows considerably more plume rise than the individual sources.

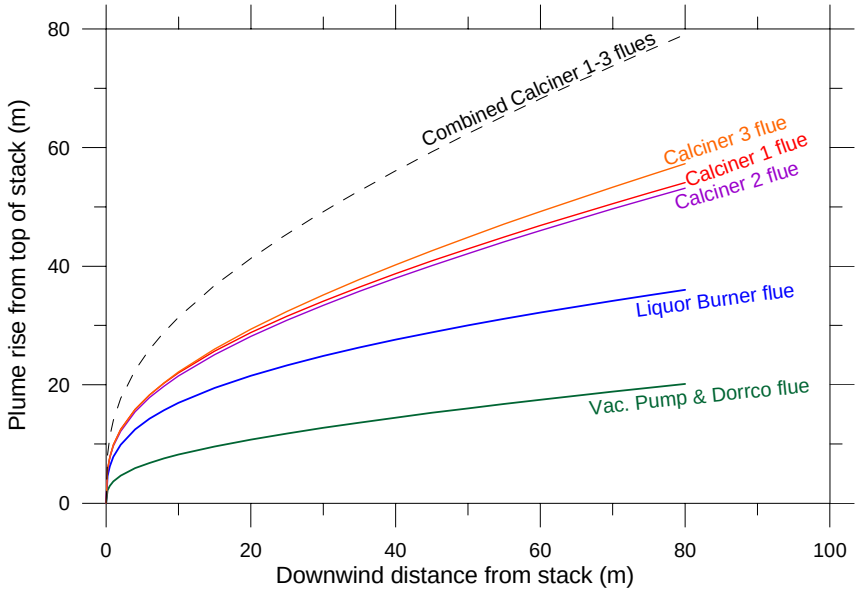

Figure A6: Plume trajectories for the plumes from the flues in the 100-m Multiflue calculated according to equation (A3) for a wind speed of 4 m s^{-1} assuming no interaction between the plumes (except for the Combined Source trajectory).

The trajectory of the Liquor Burner plume shows only one-third of the plume rise of the combined Calciner plume, and the Vacuum Pump/Dorrco plume shows only one-quarter of the rise of the combined Calciner 1–3 plume. The large differences between these trajectories make it unlikely that there will be much interaction between these plumes and so unlikely that there will be any buoyancy enhancement either between these two lower plumes or with the combined Calciner plume. The Liquor Burner and Vacuum Pump/Dorrco plumes are modelled as separate plumes, i.e. without any buoyancy enhancement.

The source radius, exit velocity and exit temperature for the three Boiler 1–3 flues are similar (see Table 1). The trajectories of the individual plumes from the Boiler stack are shown in Figure A7 for a wind speed of 4 m s^{-1} when no interaction between the plumes is assumed. These trajectories are similar, and like the Calciners 1–3 stacks, the Boilers 1–3 flues can be treated as a combined source. The trajectory for this combined source is also shown in Figure A7.

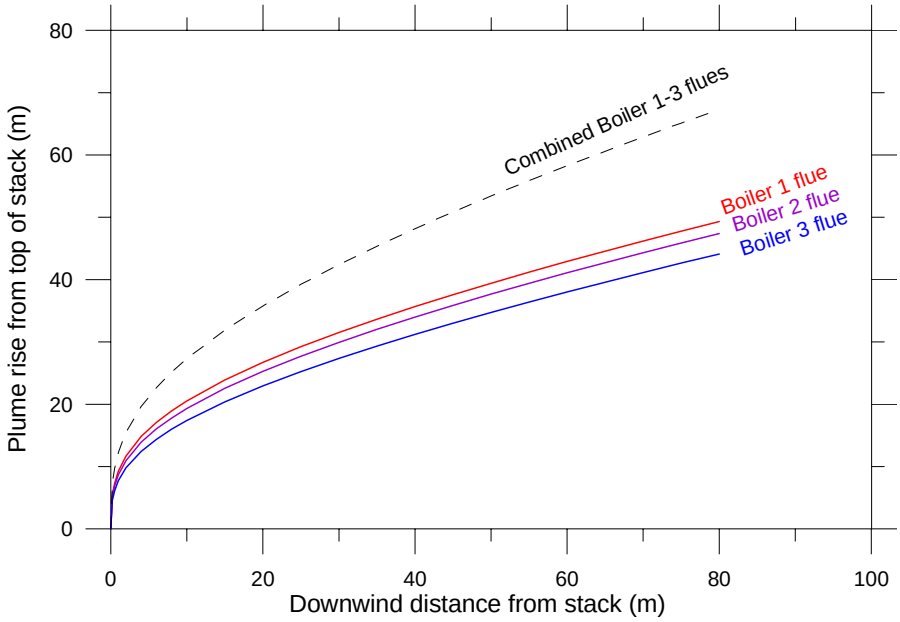

Figure A7: Plume trajectories for the plumes from the flues in the 65-m Boiler stack calculated according to equation (A3) for a wind speed of 4 m s^{-1} assuming no interaction between the plumes (except for the Combined Source trajectory).

In summary, using the method of combining sources described above, the Calciner 1–3 stacks with diameters of 1.9 m, 1.9 m, and 2.15 m, exit temperatures of 432°K, 433°K, and 469°K, and average exit velocities of 21.6 m s^{-1}, 20.8 m s^{-1}, and 19.6 m s^{-1} were modelled as a single stack with an effective diameter of 3.44 m, exit temperature of 450°K, and average exit velocity of 20.6 m s^{-1}. Similarly, the three 65-m Boiler flues with diameters of 2.4 m, 2.0 m, and 2.0 m, exit temperatures of 374°K, 397°K, and 404°K, average exit velocities of 14.5 m s^{-1}, 16.2 m s^{-1}, and 13.7 m s^{-1} were modelled as a single stack with an effective diameter of 3.71 m, exit temperature of 390°K, and average exit velocity of 14.6 m s^{-1}.

A.2.2 NO_x predictions with combined sources

TAPM was run for NO_x simulations with the Calciners 1–3 and Boilers 1–3 stacks treated as single sources, with the all other model options, including the use of the daily NO_x emission rates, the same as those used in the computations corresponding to the model results shown in Figure A5. (Note that the source data used in the ANSTO tracer modelling in Section 4.3 also used the effective source approach involving plume buoyancy enhancement for the 65-m Boiler Multiflue and the 100-m Multiflue.) The new model runs were carried out on an IBM eServer Cluster 1350 using dual 3.2 GHz Xeon processors running under the Linux operating system. The TAPM code was compiled using an Intel Fortran compiler version 8.0.

The results are presented as a q-q plot in Figure A8, showing the hourly-averaged modelled vs. observed NO_x concentrations at Upper Dam. A comparison with Figure A5 indicates that there is a substantial improvement in the model predictions when the Boilers 1–3 flues and the Calciners 1–3 stacks are treated as single sources. In Figure A8, the model distribution agrees closely with the observed distribution for the

concentration range 10–25 ppb. The model underestimates the top six concentrations. The differences between the model and observed distributions below 10 ppb are mainly because the low observed concentrations are dominated by background NO_x levels that are not constant but fluctuate, whereas the modelled concentrations assume a constant background concentration of 2 ppb. The q-q plots (not shown here) for winter, summer, daytime and nighttime for Upper Dam obtained using the combined source approach together with the daily NO_x emission rates are similar to those for Run B in Figure 12.

It can be concluded from the above NO_x comparison results that combining of closely-spaced sources with enhancement of plume buoyancy leads to better predictions than when treating such sources separately. This is consistent with international air pollution modelling practice for closely-spaced sources.

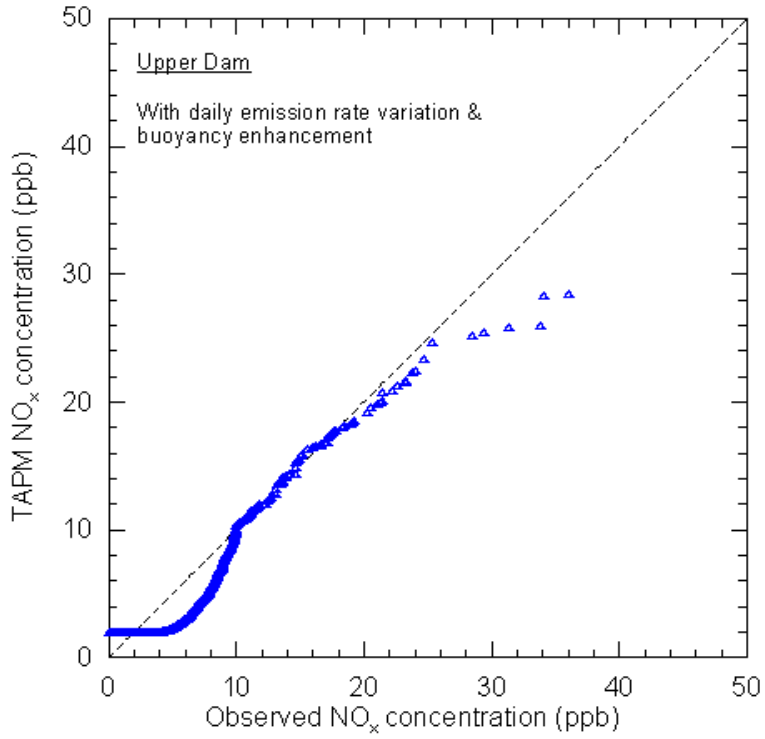

Figure A8: Quantile-quantile plots of the hourly-averaged modelled vs. observed NO_x concentrations for Upper Dam. The modelled concentrations were computed using the daily variation of the emission rates, with the 100-m and 65-m multiflue stacks combined as single stacks (i.e. full buoyancy enhancement).

Modelled and observed values of the concentration statistics for Upper Dam with plume buoyancy enhancement are given in Table A1, which show some underestimation by the model of the higher end of the concentration distribution.

Table A1. Observed and modelled statistics of NOx concentrations at the Upper Dam (sample size = 5531) monitoring sites when plume buoyancy enhancement is used in the model.

Statistic	Observed (ppb)	TAPM* (ppb)
Mean	2.2	2.4
90th percentile	4.6	2.1
95th percentile	6.4	3.4
99th percentile	13.4	13.6
Average of top ten	29.1	25.2
99.9th percentile	26.8	24.9
2nd highest	34.1	28.4
RHC	39.5	31.6
Maximum	36.0	28.5

*A background NO_x concentration of 2 ppb is added to the modelled concentrations (see Section 4.2.3).

References to Appendix A

Alcoa: 2004. Nitrogen oxides (NO_x) and carbon monoxide (CO) monitoring program report. Alcoa Wagerup Environmental Group, Alcoa World Alumina Australia, 1st edition, March 2004, 57 pp.

Anfossi, D., Bonino, G., Bossa, F., Richiardone, R.: 1978. Plume rise from multiple sources: a new model. *Atmospheric Environment* **12**, 1821–1826.

Briggs, G. A.: 1984. Plume rise and buoyancy effects. In: Randerson, D. (Ed.), Atmospheric Science and Power Production. U.S. Department of Energy, NTIS-DE84005177.

Konig, C. S., Mokhtarzadeh-Dehghan, M. R.: 2002. Numerical study of buoyant plumes from a multi-flue chimney released into an atmospheric boundary layer. *Atmospheric Environment* **36**, 3951–3962.

Manins, P. C., Carras, J. N., Williams, D. L.: 1992. Plume rise from multiple stacks. *Clean Air (Aust.),* **26** (2): 65-68.

Overcamp, T. J., Ku, T.: 1988. Plume rise from two or more adjacent stacks. *Atmospheric Environment* **22**, 625–637.